F

4046

AD A064046

LEVEL II

(9) Master's thesis,   (11) Dec 78

(12) 77 p.

(6)

EVALUATION OF ERRORS IN A
PASSIVE RING RESONATOR LASER GYROSCOPE

THESIS

(10) David J. Olkowski
~~Captain~~   ~~USAF~~

(14) AFIT/GA/EE/78-2

Charles R. Holland
~~Captain~~   ~~USAF~~

D D C

RECEIVED

JAN 31 1979

A

Approved for public release; distribution unlimited.

O12 225   JOB

79 01 30 148

EVALUATION OF ERRORS IN A

PASSIVE RING RESONATOR LASER GYROSCOPE

THESIS

Presented to the Faculty of the School of Engineering

of the Air Force Institute of Technology

Air University

in Partial Fulfillment of the

Requirements for the Degree of

Master of Science

by

David J. Olkowski
Captain   USAF

Charles R. Holland
Captain   USAF

Graduate Astronautical Engineering

December 1978

Preface

The primary objective of this thesis was to build a passive ring resonator laser gyroscope and then evaluate the performance of the gyroscope under several selected operating conditions. It is hoped that this study will aid the engineering community in analyzing the relative merits and feasibility of a passive ring laser gyro.

We wish to express special gratitude to our advisor, Maj S. R. Balsamo, for suggesting this area of research. This resourceful man devoted a great deal of his time and seemingly endless knowledge to provide us with the necessary background. His sense of humor, optimism, and determination made this experiment both successful and enjoyable.

In addition, there have been many other people who have assisted us in our endeavor. In particular, we wish to thank Mr. Robert Durham, Supervisor of the AFIT EE Laboratory, and his competent technicians, Mr. Dan Zambon and Mr. Orville Wright, for their invaluable technical advice and enthusiastic support. Also, we want to thank Mr. Carl Shortt of the Material Fabrication Shop and his personnel who provided design expertise and fabricated the actual physical components of the passive ring gyro. Another special thanks goes to Dr. Kent Stowell of the Avionics Laboratory who through his sponsorship of the project provided us with the special equipment required for this experiment.

Finally, we thank our wives, Nancy and Sue, for their continued patience, understanding, and devotion during the time we spent away from them preparing and completing this project.

Table of Contents

Table of Contents

List of Figures

List of Figures

List of Symbols

A	Resonant cavity area or mirror losses due to absorption
$\overset{\circ}{A}$	Angstrom
AMP	Amplifier
A/O	Acousto-optic Light Modulator
A(s)	Transfer function of cavity loop components
B(s)	Transfer function of cavity loop components
BS	Beamsplitter
C	Centigrade temperature
c .	Speed of light or designates cavity loop
cm	Centimeter (10^{-2} meters)
COMP	Compensator circuit
CCW	Counterclockwise
CW	Clockwise
d_+	Distance traveled in CW direction
d_-	Distance traveled in CCW direction
D/A	Digital/analogue
DET	Light Detector
DIFF AMP	Differential Amplifier
Δ'	Relates the cavity length to the frequency of the incident light
f	Frequency
f_{CCW}	Frequency in CCW direction
f_{CW}	Frequency in CW direction
f_1	Center frequency (40 MHz)
f_2	VCO frequency output
f_c	Resonant cavity frequency
f_o	Laser Frequency

List of Symbols

f_Ω	Resonant cavity frequency change due to Sagnac effect
Δf	Frequency difference $(f_1 - f_2)$
$\Delta f_{\frac{1}{2}}$	Frequency difference defined at the point where the transmission is down to half its peak value
$\Delta f_{R_{CCW}}$	Residual noise in CCW direction
$\Delta f_{R_{CW}}$	Residual noise in CW direction
δf_o	Laser jitter
δf_1	Acousto-optic noise for f_1
δf_2	Acousto-optic noise for f_2
δf_c	Cavity noise
δf_{cn}	Noise introduced by the CW and CCW common elements
δf_{CCW}	Noise introduced in the CCW direction by the non-common elements
δf_{CW}	Noise introduced in the CW direction by the non-common elements
μf	Microfarad (10^{-6} farads)
$\mathcal{F}$	Finesse
FS	Frequency Synthesizer
FSR	Free Spectral Range
G	Gain
HVA	High Voltage Amplifier
Hz	Hertz
I	Intensity signal
I_{CCW}	Intensity signal in CCW direction
I_{CW}	Intensity signal in CW direction
INT	Integrator circuit
I_o	Intensity of the incident light
I_T	Intensity of the output light
$I_{T_{MAX}}$	Maximum intensity of the output light

List of Symbols

ΔI	Intensity difference ($I_{CCW} - I_{CW}$)
KHz	Kilohertz (10^3 Hz)
L	Cavity Length
L_{CCW}	Cavity length in CCW direction
L_{CW}	Cavity length in CW direction
ΔL	Change in cavity length
λ	Wavelength of input light
LIA	Lock-in Amplifier
m	Mode number
M	Mirror
M_1	Slightly transmissive input mirror
M_o	Slightly transmissive output mirror
M_R	Mirror of reflectivity (R)
MHz	Megahertz (10^6 Hz)
mm	Millimeter (10^{-3} meters)
mW	Milliwatts (10^{-3} watts)
n	Integer
nm	Nanometer (10^{-9} meters)
Ω	Input rotation rate or measure of resistance
OSC	Oscillator
φ	Phase difference
P	Cavity perimeter
ΔP	Difference in cavity perimeter
PSD	Phase Sensitive Detector
PRG	Passive Ring Gyro
PRLG	Passive Ring Resonator Laser Gyroscope

List of Symbols

PZT	Piezoelectric Length Transducer
q	Large integer
r	Designates rate loop
R	Reflectivity or radius
T	Transmission of the mirror
t	Time
t_+	Transit time in CW direction
t_-	Transit time in CCW direction
Δt	Transit time difference $(t_+ - t_-)$
V	Volts
VCO	Voltage Control Oscillator
V_I	Detector output voltage
V_m	Modulation frequency voltage
V_o	PSD output voltage
WBA	Wideband Amplifier

Abstract

The passive ring resonator laser gyroscope is a new approach to
measuring inertial rotation. This approach is based upon the Sagnac
effect[1] and uses a passive ring Fabry-Perot interferometer as the ro-
tation sensing element. This report contains the results of a series
of tests which were accomplished on a passive ring resonator laser
gyroscope. The report contains a detailed description of this device
plus a description of each test performed. These tests include noise
measurements, inertial rotation measurements, and bias measurements.
The test results show that the relationship between the output freq-
uency and input rotation rate is linear and is consistent with pre-
viously published data[2] indicating no lock-in problem. The output
bias is shown to be affected by piezoelectric transducer position and
by differences in intensity between the counter-rotating light beams.
Additionally, the difference in intensity also is shown to affect the
noise content of the output. These significant new results lead to a
recommendation to improve the performance of this new type of gyro-
scope via the addition of an intensity feedback control loop. In ad-
dition, the distortion of the rotation sensing cavity due to length
changes in a piezoelectric length transducer shows that a cavity made
of a lower thermal coefficient of expansion material is necessary to
minimize the size of the piezoelectric length transducer and, there-
fore, the distortion due to the transducer.

I Introduction

Background

Presently, most inertial navigation units use mechanical gyros which employ a spinning mass as the rotation sensing element to stabilize the platform of the attitude reference system. However, the mechanical nature of these devices limits their performance. These devices are subject to linear acceleration and cross axis coupling errors. Additionally, the dynamic range of mechanical gyros where accurate measurements can be made is limited to about 10 revolutions per minute.[3] Therefore, the need for higher performance and reliability has prompted research for other approaches to rotation sensing. One of the more promising approaches, and one that is receiving much interest from the military, is the active ring laser gyroscope.

This laser gyro approach has progressed rapidly in the past decade. From the first work on the technique in 1963, today's technology has validated the concept with significant data and field demonstration of performance. The performance characteristics of this new approach have, in fact, proven that the laser gyroscope is an ideal candidate for many navigation, guidance, and attitude-reference applications. Use of this gyro as an inertial component offers distinct advantages over the currently used mechanical devices. These advantages include instantaneous operation, an input axis precisely defined by the lasing plane, adaptability to digital output, freedom from gravitational and acceleration errors, and a simple, rugged, low cost design.[4] The essential feature of this laser gyroscope is a

1

ring type cavity in which the laser radiation traverses a closed path. The laser cavity supports two independent, oppositely direct- ed traveling waves that can oscillate at different frequencies. The frequencies of oscillation of the traveling waves are dependent on the rotation of the cavity with respect to inertial space.[5] To bet- ter understand this important and basic principle of operation in the laser gyroscope, a review of the Sagnac effect is in order.

In 1913, Sagnac first successfully demonstrated how rotation could be measured from a difference in optical path length. Figure 1.1 shows an ideal circular interferometer. Light enters at point A and is split by the beamsplitter. In this ideal interferometer, the
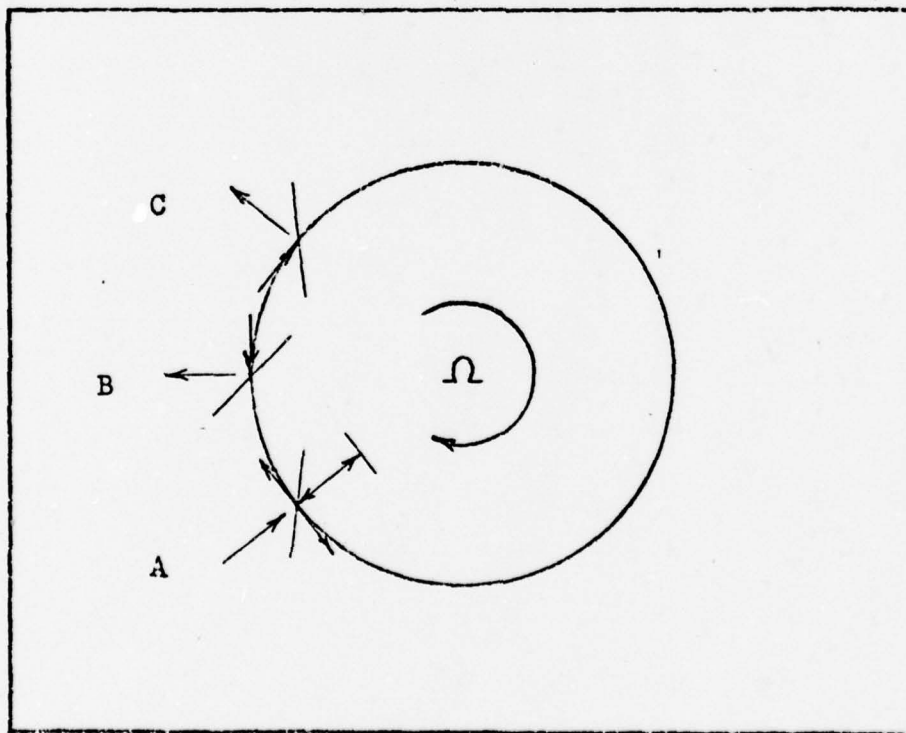

Figure 1.1 Circular Rotating Sagnac Interferometer

light is constrained to travel along the circumference of the circle. After traveling along the complete path, the light recombines at the original beamsplitter. When the interferometer is stationary, the transit time for the light to make a complete path is the same for both beams. If the interferometer is rotated at a constant speed Ω, the closed path transit time becomes different for light traveling with and against the direction of rotation.[1] This occurs because of the fact that during the closed path transit time of the light travelling clockwise (CW), the beamsplitter, originally located at A, moves to point C. The light travelling counterclockwise (CCW) meets the beamsplitter at point B. Thus, with respect to inertial space, light travelling against and with the direction of rotation must traverse a smaller and greater distance, respectively, than when there is no rotation.

Applying the concept of the Sagnac effect to the laser gyro approach, it can be shown that the difference in the optical path length of the oppositely travelling waves is related to inertial rotation by

$$\Delta L = (4A/c) \, \Omega$$

where ΔL is the difference in optical path length, A is the area enclosed by the light, c is the speed of light, and Ω is the rotation rate imposed upon the interferometer.[6] Within a ring laser cavity, an oscillation condition must be present during operation such that

$$m\lambda = L$$

where m is the mode number (an integer typically of order 10^5 to 10^6), λ is the wavelength of the light and L is the cavity optical length. Using the relationship $\lambda = c/f$ where f is the frequency of the light,

the oscillation condition becomes

$$f = mc/L$$

Therefore, a small change in L will result in a change in f so that

$$\Delta f/f = \Delta L/L$$

$$\Delta f = f \Delta L/L$$

and again using the relationship between f and λ yields

$$\Delta f = c\Delta L/\lambda L$$

Then, using the expression for ΔL, Δf is related to Ω by

$$\Delta f = (4A/\lambda L) \, \Omega$$

Therefore, a difference in the frequencies of the counter-rotating light beams results with the inertial rotation of the ring laser cavity. The rate of rotation can be determined by measuring the frequency difference between the two beams.

Current operational ring laser gyroscopes do, on the other hand, have some problems in the process of inertial rotation measurement. Since the gain medium is present within the ring cavity, these gyroscopes have errors due to the gain medium which affect the design. The major obstacle in the manufacturing and design of active ring laser gyros is the lock-in problem.

To explain this lock-in phenomenon, first the origin needs to be considered. The lock-in problem arises due to mutual coupling between the oppositely directed traveling waves. The dominant source of the coupling is the mutual scattering of energy from each of the beams, at the optical elements, into the direction of the other. As a result, when the rotation rate in the laser gyro is reduced below some critical value (called the lock-in threshold) the frequency difference between the oppositely directed traveling waves synchronizes to a common value.

Thus, for rotation rates below the lock-in threshold, the laser gyro is not responsive to rotations.[5] There are well over one hundred active ring laser gyro patents and almost all are directed to the lock-in problem.[3] Therefore, since the approach to solving the lock-in problem is one of the most important design considerations, the techniques employed by individual companies are still highly proprietary. Figure 1.2 is a graph of the results from a typical ring laser gyro.
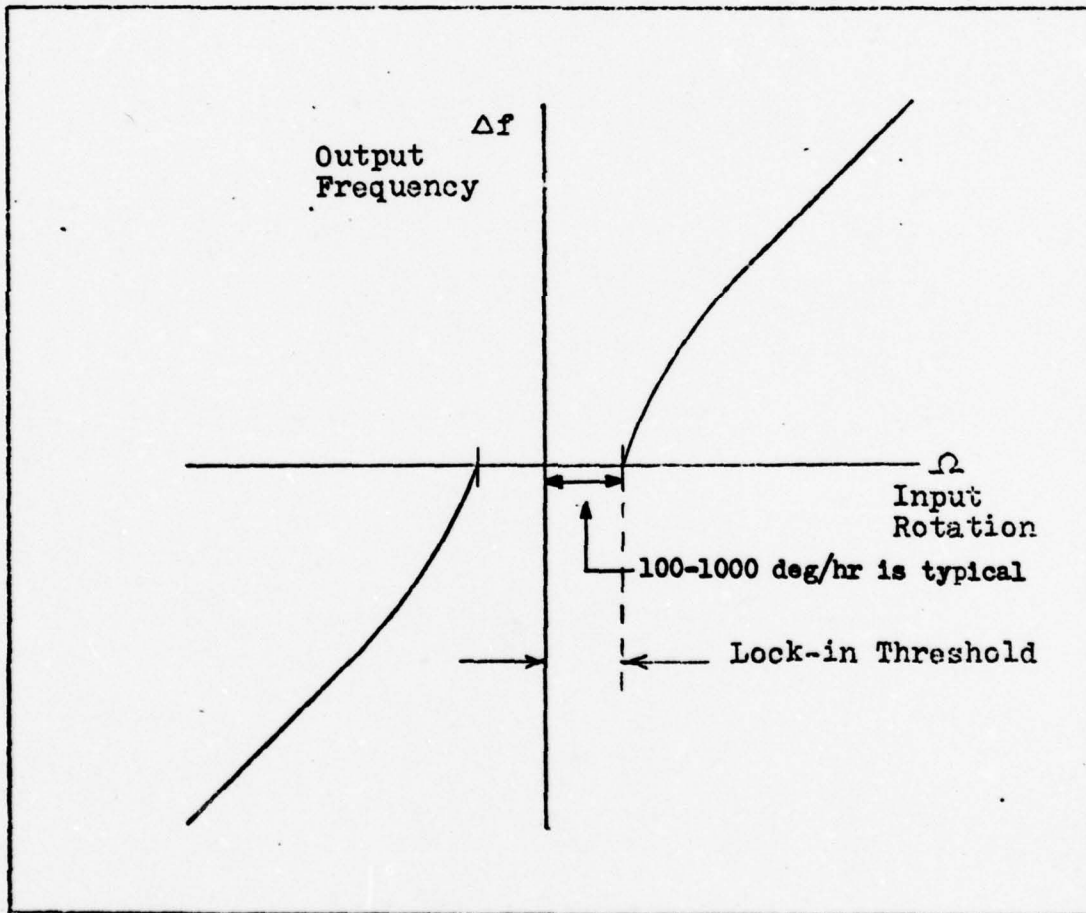
Figure 1.2 Lock-in Effects

An alternative to the active ring laser approach is the passive ring resonator laser gyro (PRLG) approach.[2] This method is free from the major problems which are attributable to the presence of the gain medium within the ring cavity since it employs a laser external to the resonant cavity. From previous research, this approach offers reliable data for input rates previously in the lock-in region. Figure 1.3 shows this comparison. It can be seen that, within the lock-in region, linear results are obtained.
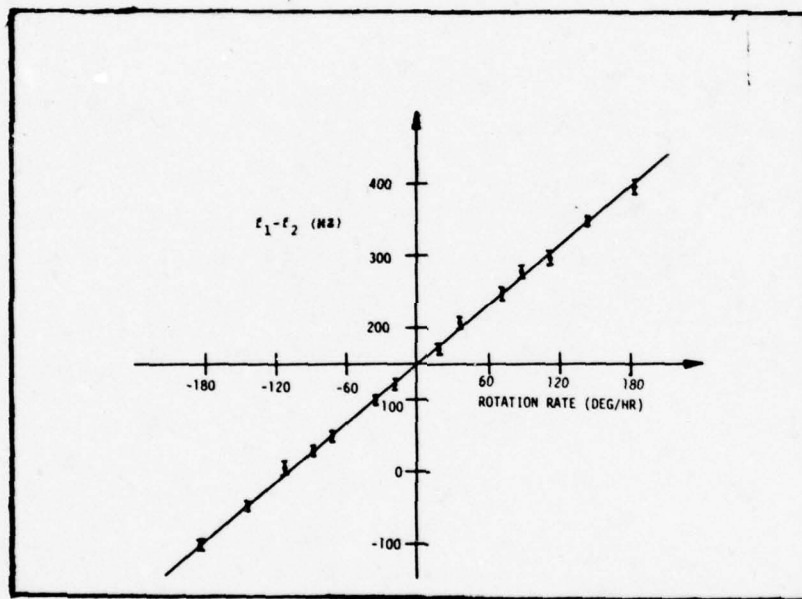
Figure 1.3 Measured Frequency Difference (Δf) as a Function of Rotation Rate Ω[2]

The passive ring laser gyro approach to inertial rotation measurement is still in its infancy compared to active ring laser development. The only published information on this approach is the previous work by S. R. Balsamo and S. Ezekiel.[2] Other than the basic concept of removing the gain medium from the inertial rotation sensing cavity, no previous effort has gone into improving the technique used to extract the inertial rotation information.

6

Problem Statement

The intent of this effort is to identify and evaluate several problems associated with the PRLG approach. A PRLG will first be built and its performance as an inertial measurement device will be demonstrated. In order to better understand the practical aspects of implementing this approach to measure rotation, several experiments will be conducted. Bias stability and inertial rotation measurements are of interest for any new inertial rotation measuring device, so these measurements will be obtained. Since a critical component of the PRLG is a piezoelectric length transducer, the effect of nonlinearities within this component will be investigated. Finally, the effect of intensity variations on noise and bias will be determined.

Whereas the active ring laser output noise is generally limited by the noise introduced due to the scheme selected to operate the gyroscope outside the lock-in region, the passive ring output noise should only be limited by the sensing detector shot noise. This investigation is necessary to examine the noise sources in the current design and, therefore, make improvements such that the fundamental shot noise limit is attained.

Method of Approach

Fundamental to the design of the passive ring gyroscope is a control loop designed such that a piezoelectric length transducer adjusts the length of a resonant cavity based upon some signal indicating the cavity's position relative to resonance. Practical experience was gained in this regard by building a laser and then locking the laser frequency to the center of the gain curve.

7

The passive ring laser gyroscope used for this thesis had to be built from basic components. This included the design and fabrication of two electronic control loops along with two detector pre-amplifiers. In addition to the electronic circuitry required, several mechanical components were designed and fabricated. Upon final assembly, the PRLG was completely checked out and minor changes, as required, were accomplished. The PRLG was then tested for performance as an inertial rotation rate sensor. Finally, a series of tests were performed exploring primarily two potential error sources. The piezoelectric length transducer was evaluated and the effects of relative intensity of the counter-rotating beams were examined.

Order of Presentation

The description and results of the PRLG experiment are presented in the following sequence. First, the passive ring gyro is discussed to include a description, operation, design, and physical characteristics of the gyro. Then a detailed description of the data measurements follows to include an explanation of the individual tests and a graphical representation of the results. Finally, in addition to closing remarks, recommendations for improvement and further study of this laser gyro are mentioned to stimulate additional research in this area.

II Passive Ring Resonator Laser Gyroscope

General Description

The principle of operation of all optical instruments used to obtain a measurement of inertially referred rotation rate is the Sagnac effect. A classical theory argument is given here as a conceptual description of this effect. Referring back to Figure 1.1, an expression can be developed for the closed path transit time for light traveling CW and CCW around a circle of radius R.

In the CW direction (the same direction as the rotation), the transit time is t_+. Then the distance traveled is

$$d_+ = ct_+ = 2\pi R + R \Omega t_+$$

In the CCW direction the distance traveled is d_- where

$$d_- = ct_- = 2\pi R + R \Omega t_+$$

Solving these equations for Δt where $\Delta t = t_+ - t_-$, to first order in $R \Omega/c$, one finds

$$\Delta t = t_+ - t_- = 4 \pi \Omega R^2/c^2$$

This implies an optical path length difference of $\Delta L = c\Delta t$ so

$$\Delta L = 4\pi \Omega R^2/c$$

But the enclosed area is πR^2 and so in general

$$\Delta L = 4A \Omega/c$$

It is this optical path length difference which is measured, thereby giving a measure of Ω which is the inertially referred rotation rate about an axis normal to the plane determined by the area A.

Early attempts to measure ΔL originated with Sagnac himself[1] and thus the instrument is called the Sagnac interferometer. This instrument measured a phase difference, φ, dependent upon the optical

9

path length difference and the wavelength of light used. That is,

$$\varphi = \Delta L / \lambda = (4A\,\Omega)/c\lambda = (4A/c\lambda)\,\Omega$$

Based upon this equation, in order to sense earth rate with a phase difference of one quarter of a wavelength, one would need an enclosed area equivalent to a square with $\frac{1}{4}$ mile on each side using visible light. Because of this low sensitivity, no further development of gyroscopes, based upon the Sagnac effect, occurred until the invention of the laser.

A very simple description of a laser is all that is necessary here for the understanding of the principle of operation of the laser gyroscope. The laser can be viewed as a light amplifier coupled with a resonant cavity such that the output frequency of the laser light is related to the length of the resonant cavity. Referring to Figure 2.1

$$2L = q\lambda \quad \text{(resonance condition)}$$

where L is the cavity length (2L is the round trip path of the light), q is a large integer and λ is the wavelength of light, but

$$\lambda f = c$$

so $\quad 2L = qc/f$

or $\quad f = q(c/2L)$

or $\quad \Delta f/f = |\Delta L/L|$

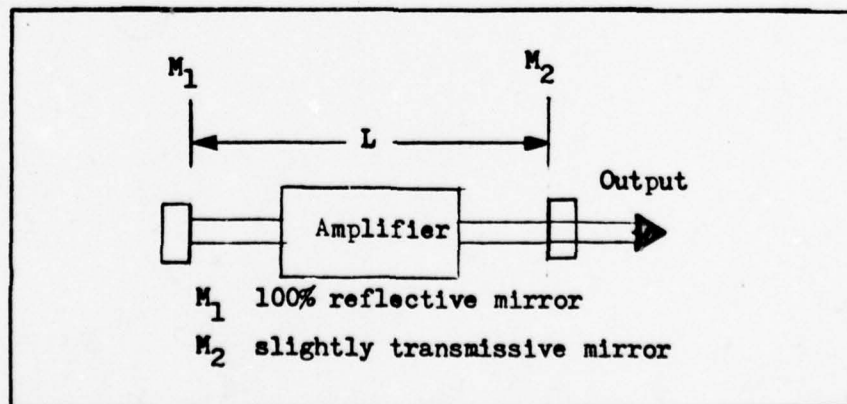Excluding the sign then $\quad \Delta f = (f/L)\Delta L$

Figure 2.1 A Two Mirror Laser

10

This relationship between a resonant cavity length change and a change in the laser output frequency is such that very small changes in cavity length make very large changes in output frequency. For example, for a cavity length of 100 cm and light in the visible range ($f \approx 10^{14}$ Hz) then

$$\Delta f = (10^{14} \text{Hz}/10^2 \text{cm}) \Delta L$$

For a frequency change of 10 Hz then

$$\Delta L = (10^3 \text{cm}/10^{14} \text{Hz}) = 10^{-11} \text{cm}$$

Rosenthal[6] in 1961 pointed this out and went to show that this relationship could be used to measure inertial rotation. In 1963, Macek and Davis[7] built a ring laser which demonstrated that the Sagnac effect could be used to measure inertial rotation with instruments of reasonable size.

The principle for the two mirror laser shown in Figure 2.1 can be extended to a ring laser as follows. As in the linear laser, the output frequency is related to the round trip path within the resonant cavity, where

$$f_{CW} = qc/L_{CW}$$

and

$$f_{CCW} = qc/L_{CCW}$$

then

$$\Delta f = f_{CW} - f_{CCW} \approx (qc/L^2) \Delta L$$

and since $q\lambda = L$

$$\Delta f = (c/\lambda L)\Delta L$$

Thus, for a ring laser shown in Figure 2.2, any optical path length difference within the resonant cavity will introduce a difference in frequencies of the counter-rotating light beams.

Recall that the Sagnac effect gives an optical path length difference and so

$$\Delta f = (c/\lambda L)\Delta L = (c/\lambda L) (4A/c) \Omega$$
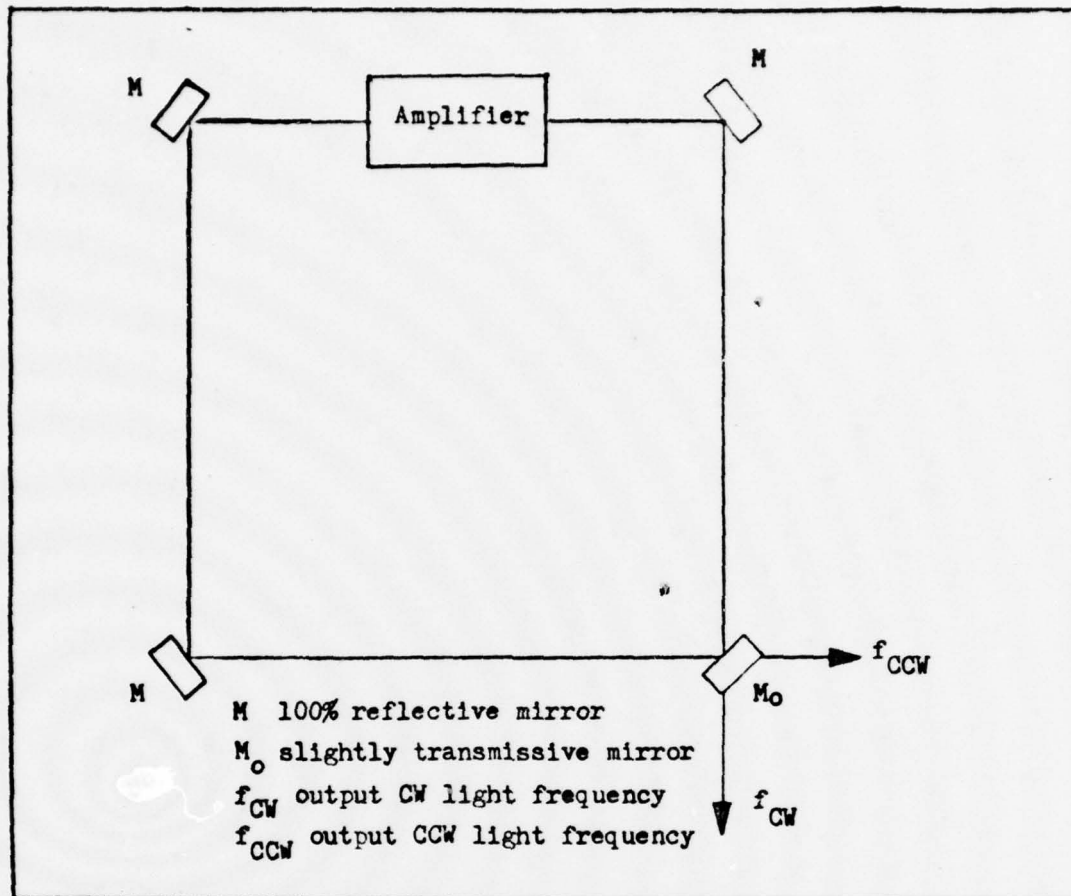
$$\Delta f = (4A/\lambda L) \Omega$$

11

Figure 2.2 Ring Laser

This expression shows that an inertial rotation rate (Ω)will introduce a beat frequency for a ring laser. In this case, for earth rate to generate a beat frequency of 10 Hz, one finds that the area must be only about 76 cm^2 assuming a square shaped ring laser operating with light in the visible region (λ = 633nm).

The active ring laser gyro has perfomed very well considering the short development time (since 1963) but it does have certain limitations as pointed out in the introduction to this thesis. This has led to another type of instrument which also senses inertial rotation rate based upon the Sagnac effect. Called the passive ring laser gyro, this instrument senses inertial rotation with the same extremely high sensitiv-

12

M   M

Amplifier

M   M$_o$ → f$_{CCW}$

M 100% reflective mirror
M$_o$ slightly transmissive mirror
f$_{CW}$ output CW light frequency
f$_{CCW}$ output CCW light frequency

↓ f$_{CW}$

ity as the active ring laser gyroscope but does not have any gain media (light amplifier) within the inertial rotation rate sensing cavity. The concept is not new and was, in fact, introduced by Rosenthal in his original paper in 1961. Probably because of the initial success of the active ring laser gyroscope, no published work related to this concept was shown until 1977.[2]

As an aid in understanding the passive ring laser gyro concept, the operation of the gyroscope is developed first by a discussion of the Fabry-Perot interferometer. This interferometer can be viewed as no more than an empty optical cavity (see Figure 2.3). The out-

I_o intensity of the incident light
L   length of the cavity
I_T intensity of the output light
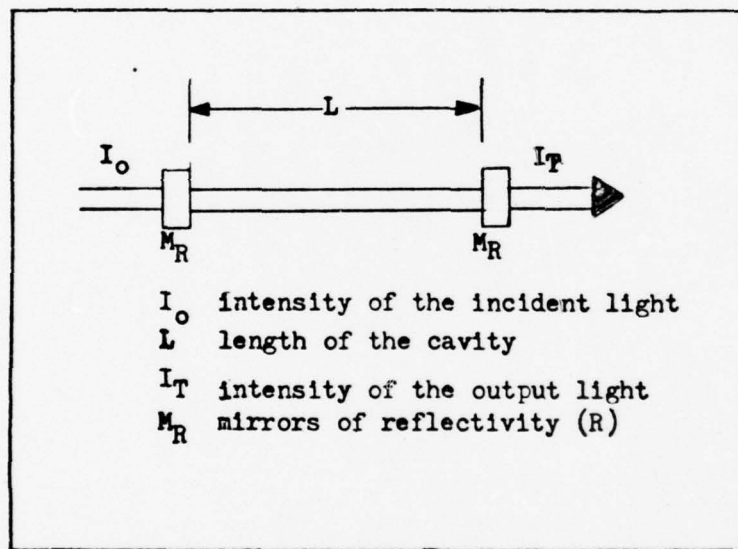M_R mirrors of reflectivity (R)

Figure 2.3   Two-Mirror Fabry-Perot Interferometer

put intensity is determined by the relationship of the resonance condition of the cavity to the frequency of the incident light. It can be shown that

$$I_T = I_o \frac{T^2}{(1-R)^2} \times \frac{1}{1 + [4R/(1-R)^2] \sin^2(\Delta'/2)}$$

where T is the transmission of the mirror, R is its reflectivity, and A is its absorption losses such that R+T+A=1.[8] For fixed R, T, and A,

13

the quantity controlling the transmission is Δ', and Δ' relates the cavity length to the frequency (or wavelength, $c = \lambda f$) of the incident light. Neglecting the phase change at the mirrors, the resonance condition is

$$\Delta'/2 = n\pi = kL \quad \text{where} \quad k = 2\pi/\lambda$$

so $\quad \Delta'/2 = 2\pi L/\lambda$

Thus we have a resonance condition for

$$2L/\lambda = n \quad \text{or} \quad L = n(\lambda/2)$$

The output intensity drops off rapidly for a slightly off resonance condition, especially for $R \approx 1$. From the Fabry-Perot transmission eq-
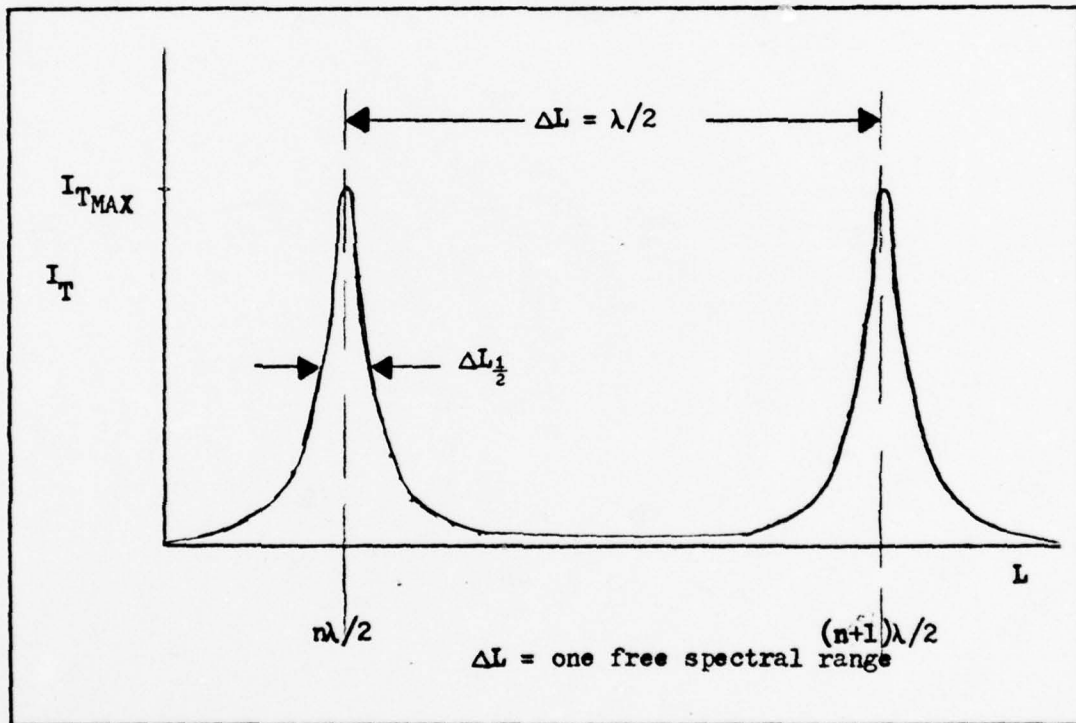

Figure 2.4 Fabry-Perot Transmission

uation for $\sin(\Delta'/2) = 0$, the transmission $I_T = I_{T_{MAX}} = I_o(T^2/(1-R)^2)$.

A measure of the quality of the Fabry-Perot is obtained by determining the width of the resonance line and relating it to the wavelength of the incident light. Then for

$$\Delta L = \lambda/2, \quad \text{FSR} = \text{one free spectral range}$$

and
$$\text{FSR} = f\Delta L/L = f\lambda/2L = c/2L$$

and, finally, the finesse, $\mathcal{F}$, relates the line width to the FSR by

$$\mathcal{F} = \text{FSR}/\Delta f_{\frac{1}{2}} = \pi R/(1-R)$$

The analysis for the two mirror Fabry-Perot interferometer is easily extended to a ring Fabry-Perot interferometer where the perimeter of the ring is related to the length of the two mirror interferometer by $P = 2L$. Thus, for a ring (see Figure 2.5) the same equations hold, but now there are in fact two interferometers, one in each direction; thus,
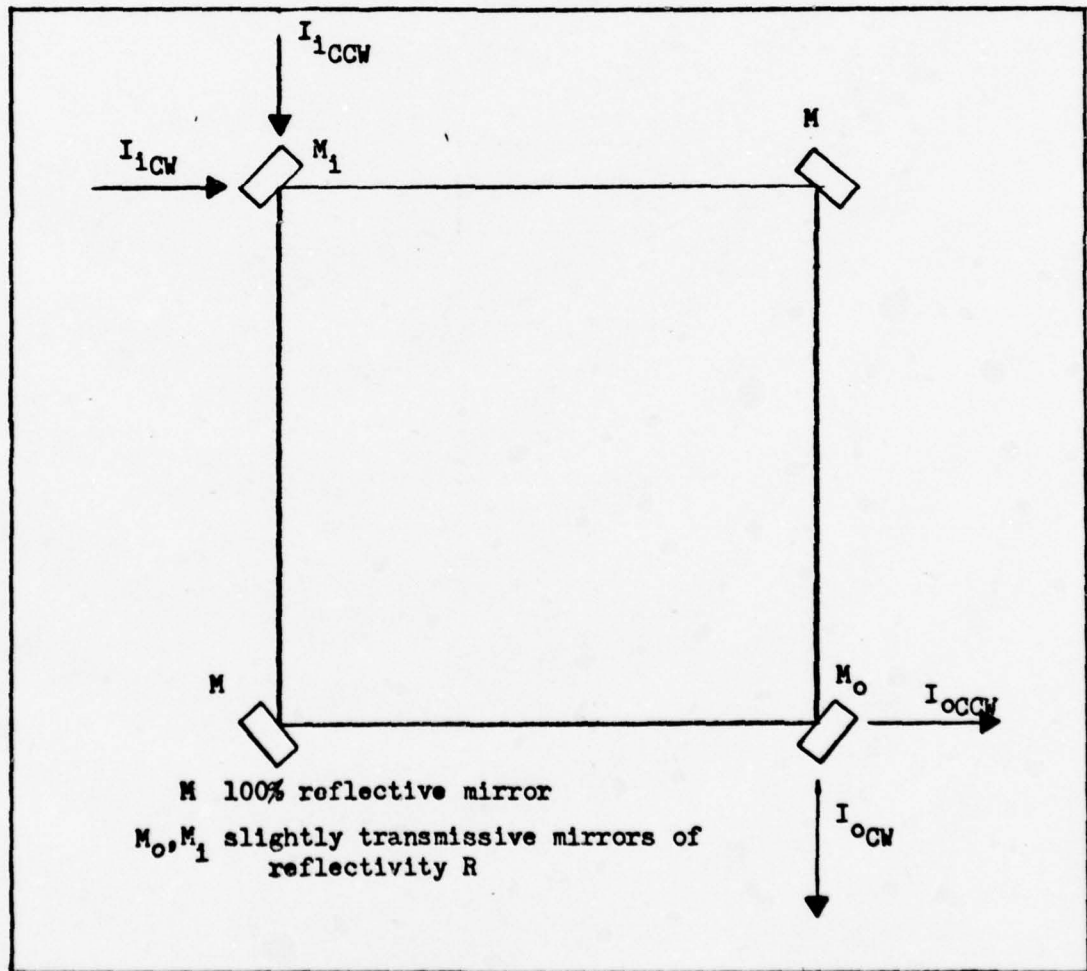

M   100% reflective mirror

M_o, M_1 slightly transmissive mirrors of reflectivity R

Figure 2.5 Ring Fabry-Perot Interferometer

15

referring to Figure 2.5, the output intensity in the CW direction, I_{oCW}, is related to the frequency of the incident light in that direction relative to the cavity resonance condition. Therefore, for a fixed incident light frequency the cavity length could be adjusted to maximize the output intensity. Similarly, for a fixed cavity length, the frequency of the incident light could be adjusted to maximize the intensity of the output. Based upon these relationships the passive ring laser gyroscope can be described.

The basic intent of the passive ring laser gyroscope is to adjust the length of the resonant cavity such that it is in resonance with the frequency of the light in one direction (say f_a) and then to adjust the frequency of light in the other direction (f_b) such that the cavity is also in resonance with f_b. If the optical path length were the same in both directions then $f_a = f_b$ and $\Delta f = f_a - f_b = 0$. But, if the optical path length were different then

$$\Delta f = f_a - f_b = f\Delta P/P \qquad (P = \text{cavity length})$$

and if ΔP were due to the Sagnac effect then

$$\Delta f = (f4A/cP)\,\Omega = (4A/\lambda P)\,\Omega$$

which is exactly the same scale factor as the active ring laser gyroscope.

Using a 1 milliwatt single frequency laser as the light source, the fixed frequency light is incident to a ring Fabry-Perot cavity and the intensity of the output is sensed. For this project a four mirror ring cavity is used with one mirror mounted on a piezoelectric length transducer which is used to control the length of the resonance cavity (see Figure 2.6). Standard modulation techniques are used, that is the cavity length is modulated such that a directional error signal is derived to drive the cavity length to the top of the resonance peak.
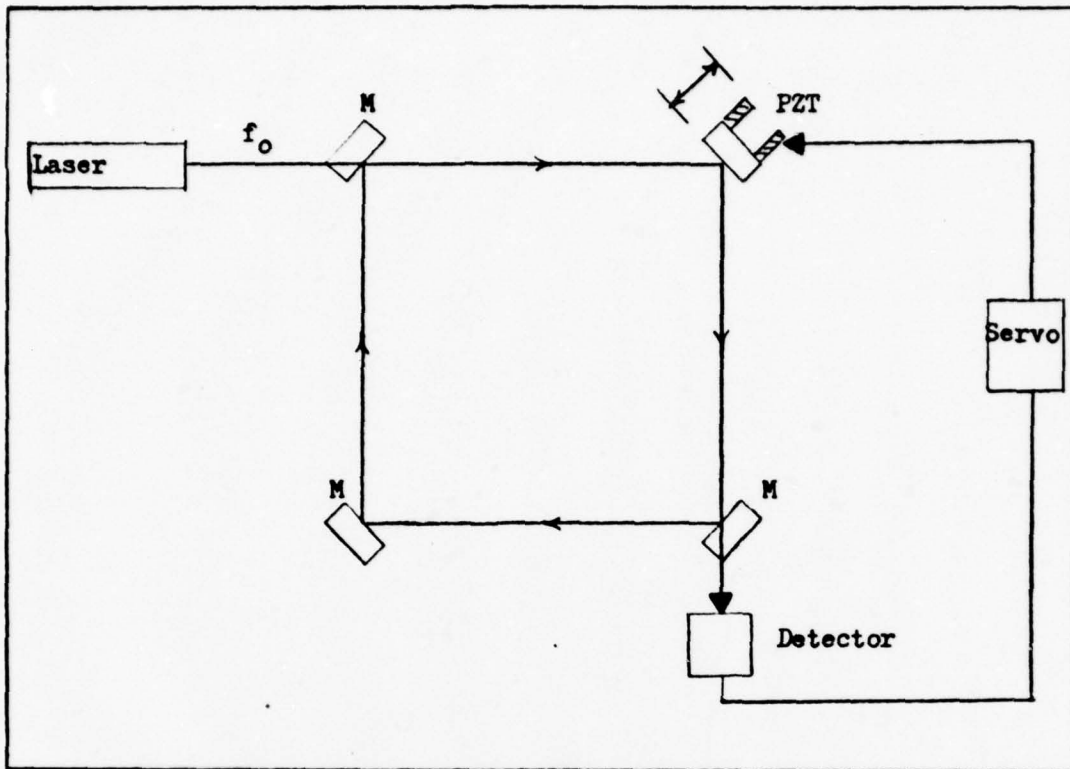
Figure 2.6 Cavity Length Control Loop

Introducing the same light frequency in the opposing direction
would generate an error signal in that direction which could be relat-
ed to the optical path length difference within the cavity and, there-
fore, inertial rotation rate. This would provide a simple open loop in-
strument. The intent of the passive ring laser gyroscope is to provide
the difference frequency directly, but for small rotation rates this
would require adjusting the incident light frequency by a few Hertz, and
at present no device is available to do this. An acousto-optic modula-
tor is available but shifts the light frequency very precisely in the
1 MHz to 1 GHz range. This device was selected for use in the passive
ring laser gyroscope. Thus in the direction controlling the cavity
length the laser frequency is shifted up by 40 MHz so

$$f_{CW} = f_o + f_1$$

17

where f_{CW} = incident light frequency in the CW direction and f_1 = 40 MHz fixed frequency and is used to control the cavity length.

In the CCW direction the incident light frequency is also shifted up by about 40 MHz (f_2) but the exact amount is determined by an error signal derived from detecting the light intensity in the CCW direction (see Figure 2.7).
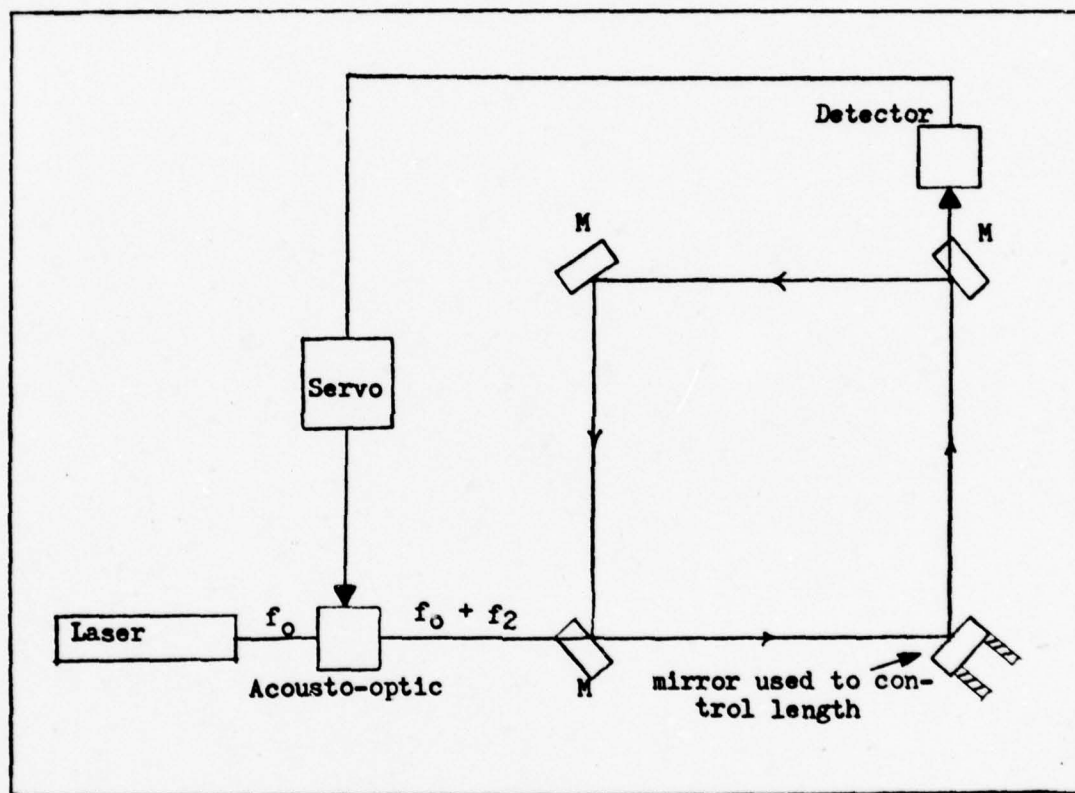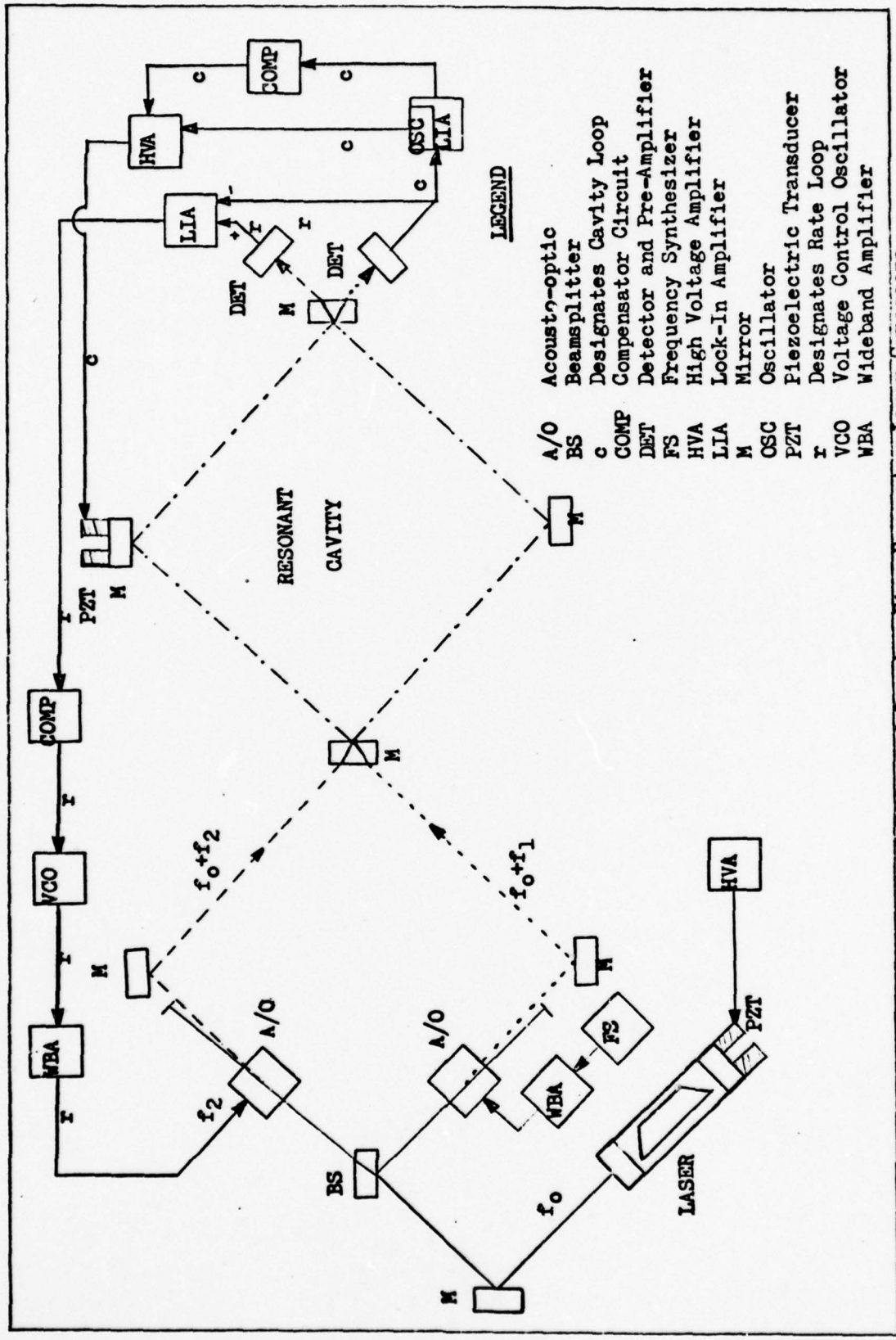

Figure 2.7 Rate Control Loop

The cavity is already modulated to provide the error signal to the cavity control loop thus the same modulation detection technique is used to derive the rate control loop error signal. The entire schematic diagram is shown in Figure 2.8. The output is then

$$\Delta f = f_1 - f_2 = (4A/\lambda P)$$

Noise resulting from the laser and cavity jitter with this scheme

18

Figure 2.8 Schematic Diagram of Passive Ring Resonator Laser Gyroscope

should be completely correlated if both beams are aligned perfectly and the incident beam intensity in each direction are equal.

In the final design the detected intensity output in the cavity control loop direction is subtracted from the intensity in the rate control loop prior to the generation of the error signal in that direction. This allows a substantial reduction in input noise for that loop. The modulation technique used in the control loops is described in Appendix A. The control diagram for the passive ring laser gyroscope used in this project is shown in Figure 2.9. No noise sources are shown in the diagram.
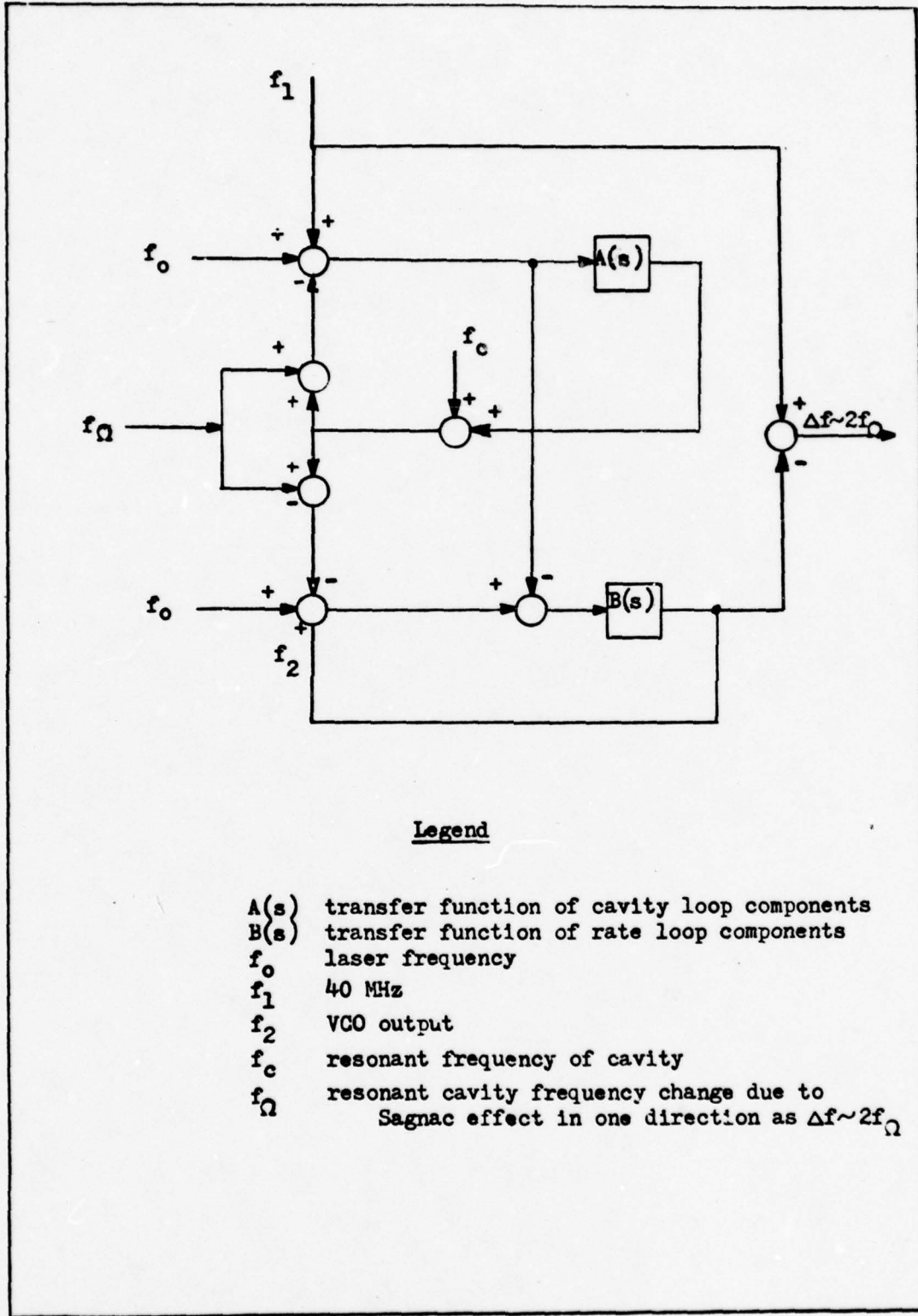
Legend

$A(s)$	transfer function of cavity loop components
$B(s)$	transfer function of rate loop components
f_o	laser frequency
f_1	40 MHz
f_2	VCO output
f_c	resonant frequency of cavity
f_Ω	resonant cavity frequency change due to Sagnac effect in one direction as $\Delta f \sim 2f_\Omega$

Figure 2.9 PRLG Control Diagram

Mechanical Design

The most extensive task in this experiment is to design and build a PRLG. To accomplish this, mounting fixtures are fabricated for the laser, mirrors, beamsplitter, resonant cavity, PZT, and acousto-optics in order that the complete assembly can be bolted to a single stabilizing mount. In this section, the individual mounting designs for the above components will be briefly explained.

The stainless steel laser mount is designed with a 23 cm cavity length using Invar rods. Due to the low coefficient of thermal expansion of Invar, this material reduces the effects of temperature variations on the cavity path length. For the initial alignment of the laser, minor adjustments in the PZT mirror are made by shimming the PZT mount. On the output end of the laser mount, an adjustable mirror mount is located in order to maximize the light intensity of the beam.

The aluminum mirror and beamsplitter mounts are designed in two parts. One part supports and allows for the adjustment of the mirror and beamsplitter through a screw and spring assembly. The other part is designed to bolt the assembly to the mounting block.

The acousto-optic mounts are simply two small stacked and attached aluminum slabs of which one of the slabs affixes to the mounting block. The other slab attaches to the acousto-optic and is designed to permit minor adjustments of the component.

The resonant cavity is made of solid aluminum, measuring 21.08 cm on a side with curved mirrors fitted on each corner where one of the cavity mirrors is mounted on a PZT. A groove is channeled out

22

within the block to support the counterrotating beams of light. The
cavity itself bolts directly to the mounting block.

The aluminum PZT mount is made to completely house the PZT. The
PZT is secured inside the mount and a mount is directly attached to
both the laser and passive resonant cavity.

The mounting block is a 61 x 45.7 x 2.5 cm solid block of aluminum.
This block is drilled and tapped to accomodate the above components. The
mounting block with the components is shown in Figure 2.10.
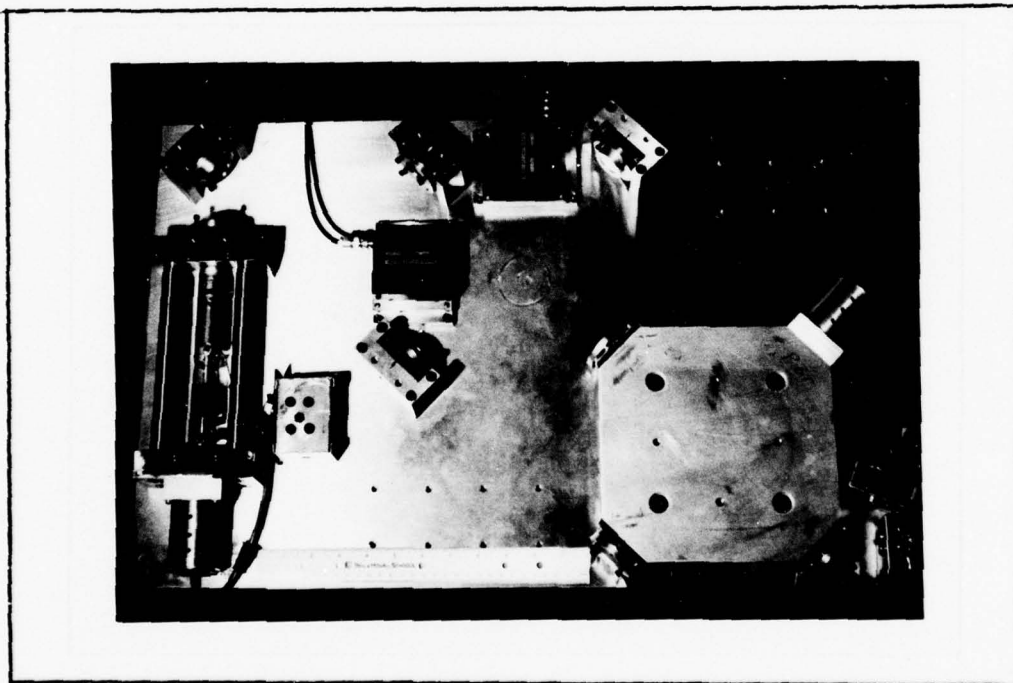

Figure 2.10 PRLG Assembly

Physical Characteristics

The two critical components of the passive ring gyro are the ex-
ternal laser and resonant cavity. To promote an increased understand-
ing of how this gyro operates, it is important to discuss the physical
characteristics of these two components.

23

External Laser. The gain tube used in this project is a C.W. Radiation
Inc. *Helium-Neon* tube. Because the mirrors used to form the laser cav-
ity are non reflective to infrared radiation, the laser output is prim-
arily in the visible region at 6328 $\overset{\circ}{A}$. For normal operation of the pas-
sive ring gyro, the external laser is required to have only one longit-
udinal mode appearing within the width of the gain curve. This spec-
ification is important to minimize mode interactions which can give rise
to spurious low frequency oscillations and noise, and completely mask
the rotation signal.[5] For this particular laser, the cavity length is
designed at 22.86 cm which according to the expression

$$f = c/2L$$

yields a longitudinal mode spacing of 656 MHz. By monitoring the laser
output on an oscilloscope, the gain curve width is determined to be 1284
MHz which verifies that mode interactions are, in fact, minimized in
this laser design. Figure 2.11 shows this relationship. In addition,
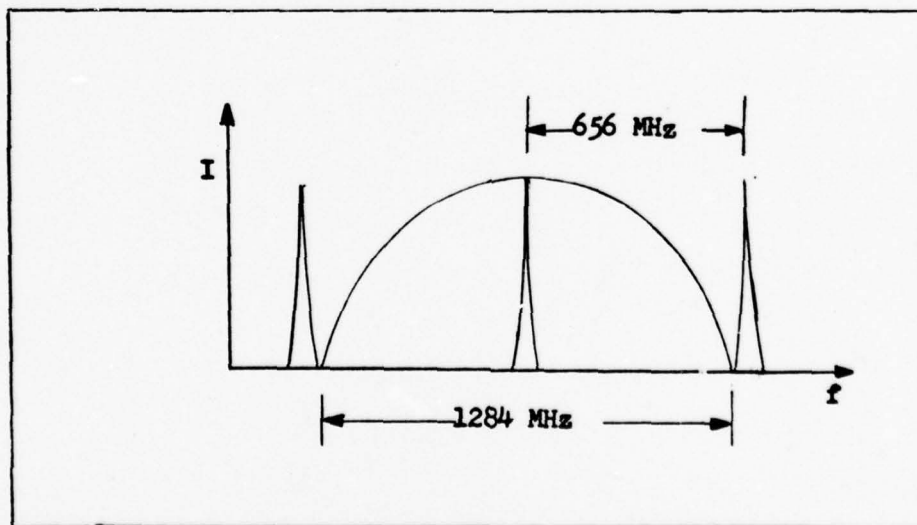the light intensity was measured at 1.43 milliwatts single frequency
output.

Figure 2.11 Laser Mode and Gain Curve

Resonant Cavity. The resonant cavity forms a ring Fabry-Perot inter-
ferometer. Of the four mirrors which form this cavity, two are approx-
imately 99% reflective (the input and output mirrors). The other two
are 100% reflective. All mirrors are curved with a radius of curvature
of 1 meter. The mirrors are aligned so that the path of the input light
forms a square of approximately 17.5 cm on a side. The free spectral
range (FSR) is found from

$$FSR = c/P$$

where c is the speed of light and P is the perimeter of the light path.
From this expression the FSR is found to be 428 MHz. The finesse, $\mathcal{F}$,
which is used as a measure of the resolution of a Fabry-Perot interfer-
ometer is obtained from the expression

$$\mathcal{F} = FSR/\Delta f_{\frac{1}{2}}$$

where $\Delta f_{\frac{1}{2}}$ is the frequency difference defined at the point where the
transmission is down to half its peak value. From the slow scan data
provided in Figure 2.12, $\mathcal{F}$ is calculated to be 145. The theoretical val-
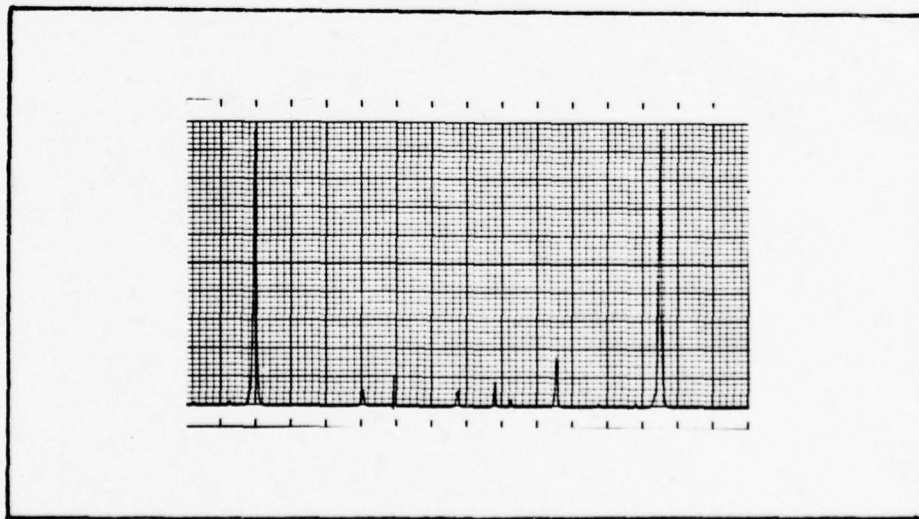
Figure 2.12 Slow Scan of Cavity Laser Modes

ue can be found by using

$$\mathcal{F} = \pi R^{\frac{1}{2}}/(1-R)$$

where R is the reflectivity of the input and output mirrors.[7] Using

an expected R = 98.98% to account for 0.02% absorbtion losses, $\mathcal{F} \approx 306$.

To obtain a finesse of approximately 145, R = 97.86%. The difference

between the reflectivities can be due to contaminants on the mirrors

which will increase the absorbtion losses. Also, the finesse formula

assumes perfect alignment of the Fabry-Perot interferometer. Any

slight misalignment of one of the four mirrors will decrease the fi-

nesse.

III Performance Investigation Results

The experiments in this project involved noise, bias, inertial
rotation, and PZT position error measurements. Prior to each test, the
PRLG was initialized using the procedure explained in Appendix A. In
addition, the PRLG was isolated thermally by placing styrofoam insul-
ation on the top and sides of the gyro. Also, a temperature control
unit was configured inside the gyro to aid in temperature stabilization.
This unit maintained the temperature within the cavity at 57°C $\pm$ 1°C.

Inertial Rotation Measurements

This test was performed by rotating the PRLG about its input axis
using the Genisco rate turn table. Rotation rate inputs from 0.1 deg/
sec to 1 deg/sec in 0.1 degree increments in both directions were used.
Data was obtained by recording the VCO output (f_2), and then subtract-
ing this from f_1 (40 MHz) plus the bias at the time of the test. Inte-
gration time was set at 10 seconds. The results are shown in Figure 3.1.

The expected slope of the output is found by

$$\Delta f = (4A/\lambda P)\ \Omega$$

In this case, the path length from mirror to mirror was measured at
17.5 cm. The 6328 $\mathring{A}$ transition of the laser was used so

$$\Delta f = [4 \times (17.5cm)^2]/[6328\mathring{A} \times 4 \times 17.5cm] \times [1\mathring{A}/10^{-8}cm] \times$$
$$[\pi rad /180deg] \times \Omega$$

$$\approx 4827\ \Omega$$

where Δf is in Hz if Ω is in deg/sec.

The results show that this design does, in fact, detect rotation
and that the relationship between Δf and rotation is linear. Further-
more, at least down to the 500 Hz level, lock-in is not present. Mea-
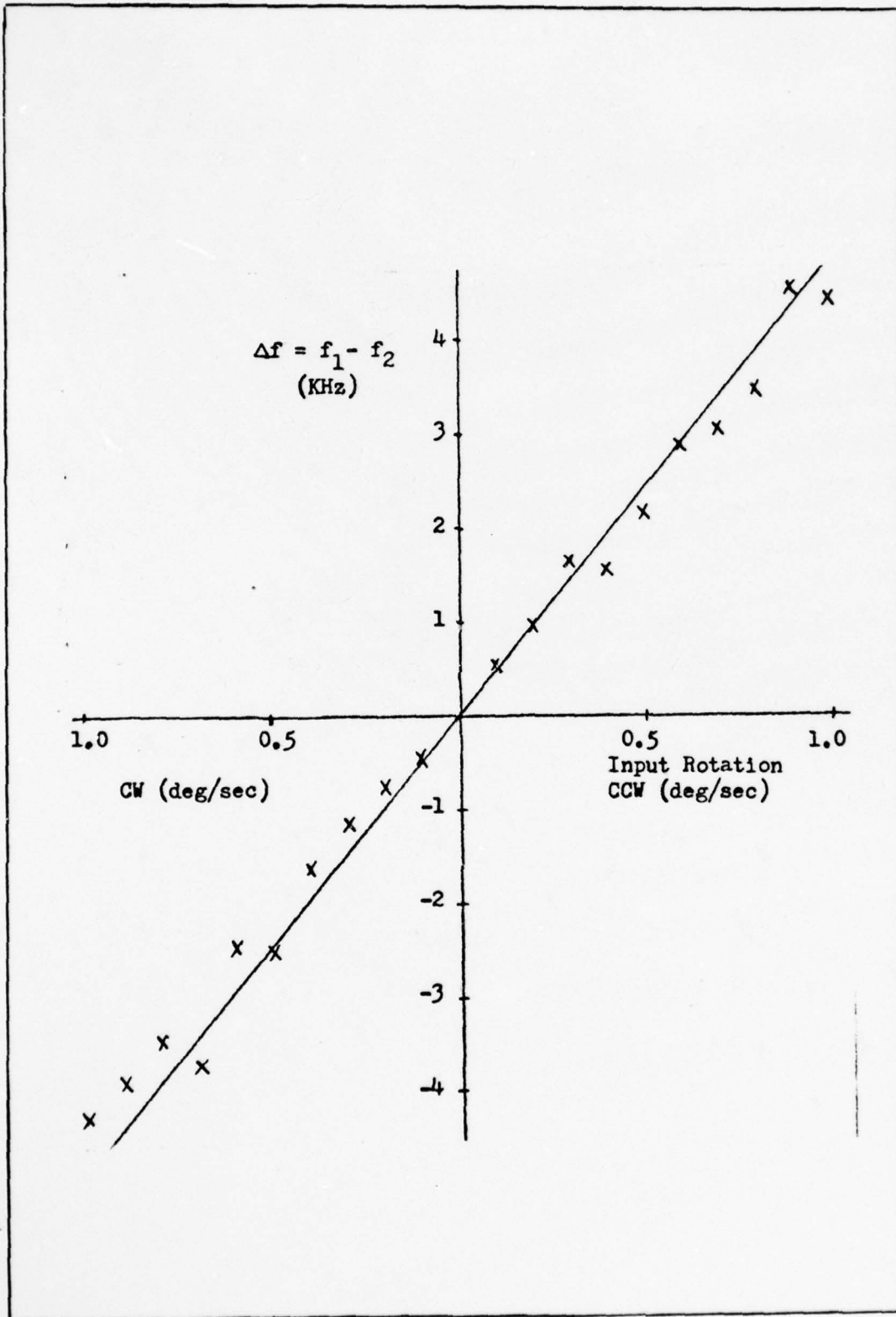
27

Figure 3.1 Δf Versus Input Rotation

surements below this level were not made because bias instability and output noise were too severe for meaningful results. No further rotation rate measurements were taken since the primary purpose of the project is to explore potential error sources of the PRLG.

Bias Measurements

Two bias measurement tests were accomplished. One was to determine the long term stability of the gyro whereas the other determined the bias change due to ΔI variations.

<u>Long Term Bias Stability</u>. This experiment is intended to show the stability of the bias over a long period of time. With no rotational input, the output of the VCO was recorded. The frequency sampling integration time was set a 1 second. The results are shown in Figure 3.2.

This test lasted 36 minutes. As can be seen, the bias is affected by a low frequency noise which peaks in approximately every seven minutes which is a frequency of approximately 0.0024 Hz. However, a recurring, relatively constant level is apparent. Its value starts at approximately 400 Hz and is 500 Hz at the conclusion of the test. This corresponds to a 3.61×10^{-4} rad/sec drift over a period of 36 minutes. The low frequency noise amplitude is approximately 400 Hz magnitude.

The bias in the PRLG is due to misalignment of the two counter-rotating beams and should be constant. No conclusive data was obtained to indicate the specific source for the bias drift or the low frequency oscillations. Thermal changes throughout the experiment cause cavity length changes and laser frequency changes which require the piezoelectric transducer to change, thereby contributing to the bias changes. In addition, bias can be caused by adjacent higher order resonant cavity modes introducing an unequal pulling effect on the fundamental resonance mode.
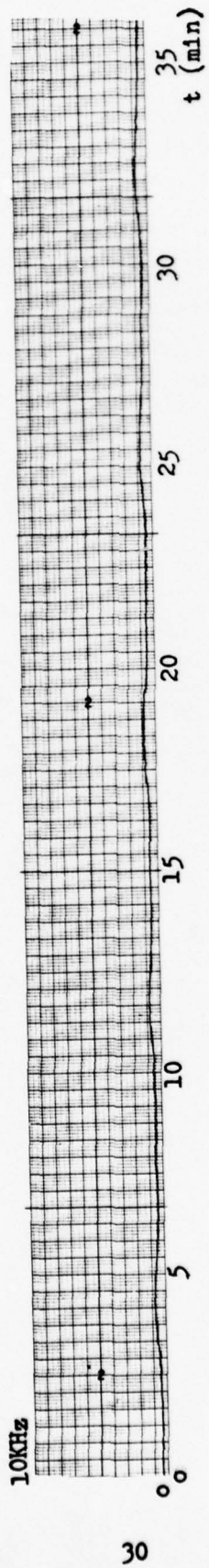
Figure 3.2 Long Term Bias Drift (integration time, τ = 1 sec)

Intensity Variation Bias. The purpose of this test is to determine
how changes in the intensity difference, ΔI, affect the gyro bias. In
this experiment, ΔI was varied from the minimum noise position, in 5 mV
increments, to $\pm$ 25 mV by the output signal amplitude knob on the VCO.
The 5 mV increment was set by monitoring the ΔI output on the chart re-
corder. Integration time for the run was set at 10 seconds and for each
setting the bias was allowed to stabilize over a 5 minute period. From
the recorder, the bias shift was apparent with the change in ΔI. The
graph in Figure 3.3 shows how variations in ΔI affect gyro bias.

Noise Measurements

The objective of this experiment is to evaluate the noise magnit-
udes in the intensity outputs and to determine the noise correlation
when the intensity difference, ΔI, is varied $\pm$ 24 millivolts (mV) in
8 mV increments. This data is obtained by displaying the desired out-
put on an oscilloscope and measuring the peak to peak value. From the
oscilloscope display, the noise measurements for the various settings
can be computed. The signal monitor output of the rate loop LIA was
used to determine noise content. This output is the output of the LIA
pre-amplifier before the phase sensitive detector. Figure 3.4 shows a
block diagram of the signals used.

The results of this experiment showed a peak to peak noise mea-
surement of 65 mV for each intensity signal. In the A - B position
$(I_{CCW}-I_{CW})$, a value of 4 mV peak to peak was obtained for the noise.
This implies an improvement in the signal to noise ratio of approxima-
tely 16 when the intensity signals are differenced. This indicates
that a majority of the noise from the two light detectors is recipro-
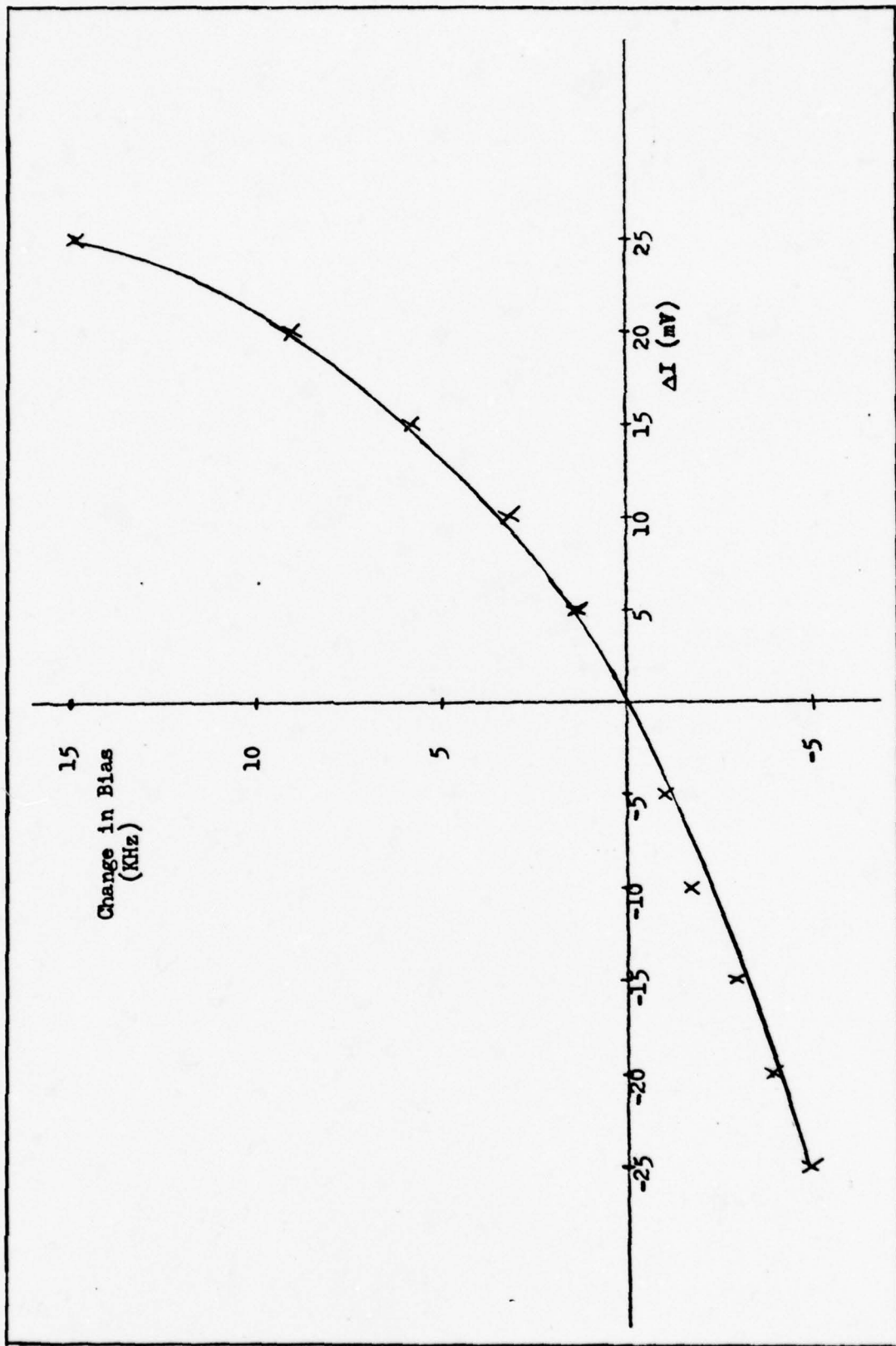cal and cancels out when the two signals are subtracted. This is so

31

Figure 3.3 Change in Bias Versus ΔI

32
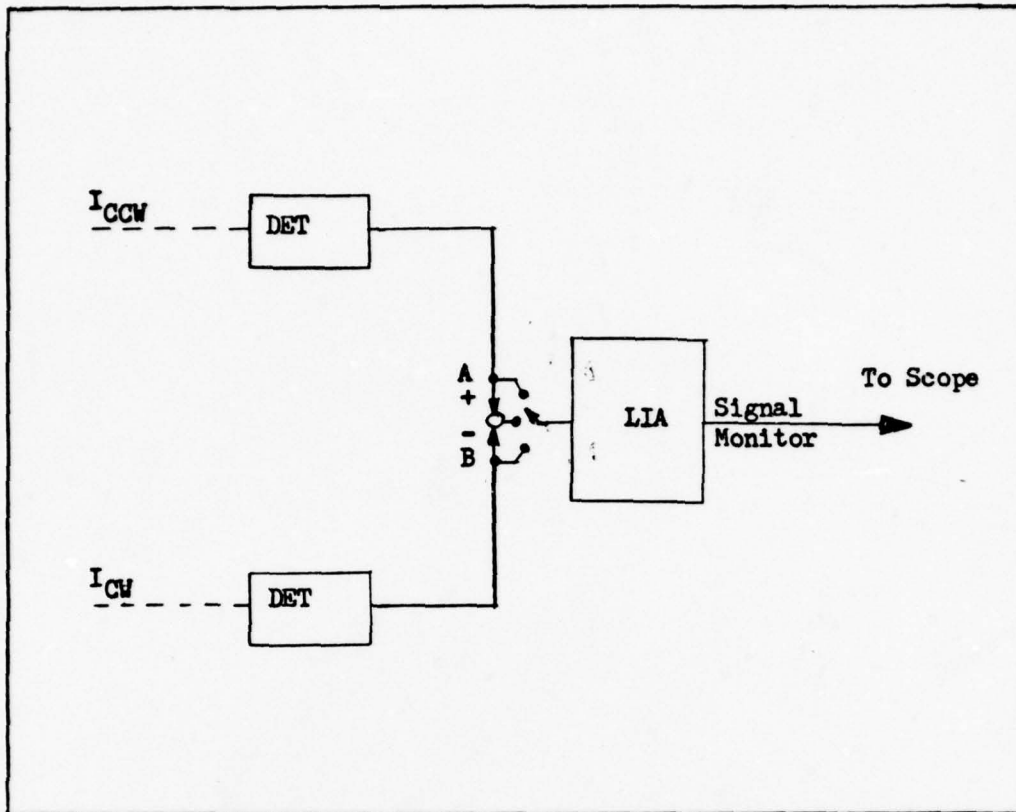
Figure 3.4 Intensity Noise Signals

because essentially all of the components in the instrument are common

to both beams. Thus, if we consider the CW resonant frequency, for ex-

ample, it will have the following components

$$f_{CW} = f_o + \delta f_o + f_1 + \delta f_1 + \delta f_c + \delta f_{cn} + \delta f_{CW}$$

where f_o is the DC laser frequency,

δf_o is the laser jitter,

f_1 is the frequency added by the acousto-optic,

δf_1 is the acousto-optic noise,

δf_c is the cavity noise,

δf_{cn} is the noise introduced by the remaining common elements,

and δf_{CW} is the noise introduced by the remaining non-common elements.

The residual noise then

33

$$\Delta f_{R_{CW}} = f_{CW} - (f_o + f_1)$$
$$= \delta f_o + \delta f_1 + \delta f_c + \delta f_{cn} + \delta f_{CW}$$

can be significant. The cavity control loop adjusts the cavity length such that $\Delta f_{R_{CW}}$ is minimized, but noise will still exist beyond the bandwidth of the loop. The rate loop takes the difference signal from the CW and CCW detectors in an attempt to further reduce this noise contribution to the measurement. For the CCW resonant frequency, f_{CCW}, the noise components are

$$f_{CCW} = f_o + \delta f_o + f_2 + \delta f_2 + \delta f_c + \delta f_{cn} + \delta f_{CCW}$$

where f_2 is the frequency added by the CCW acousto-optic,

δf_2 is the acousto-optic noise,

δf_{CCW} is the noise introduced by the remaining non-common elements. Then the difference signal will only have noise contribution from

$$\Delta f_{R_{CW}} - \Delta f_{R_{CCW}} = \delta f_1 - \delta f_2 + \delta f_{CW} - \delta f_{CCW}$$

Next, ΔI was varied from its initial position by the output signal amplitude knob on the VCO to determine the noise relationship. The results for this test are shown in Figure 3.5 which provides the noise output as a function of ΔI. As can be seen, maintaining ΔI at the minimum noise position is important for reducing noise effects due to ΔI.

PZT Error

A major cause of bias is relative misalignment of the resonant cavity. The piezoelectric length transducer, being an integral part of the cavity, is a likely candidate as a cause of misalignment and, therefore, gyroscope bias and bias changes.

The PZT position error tests were accomplished by locking the incoming light frequency to each of the cavity resonances within the full
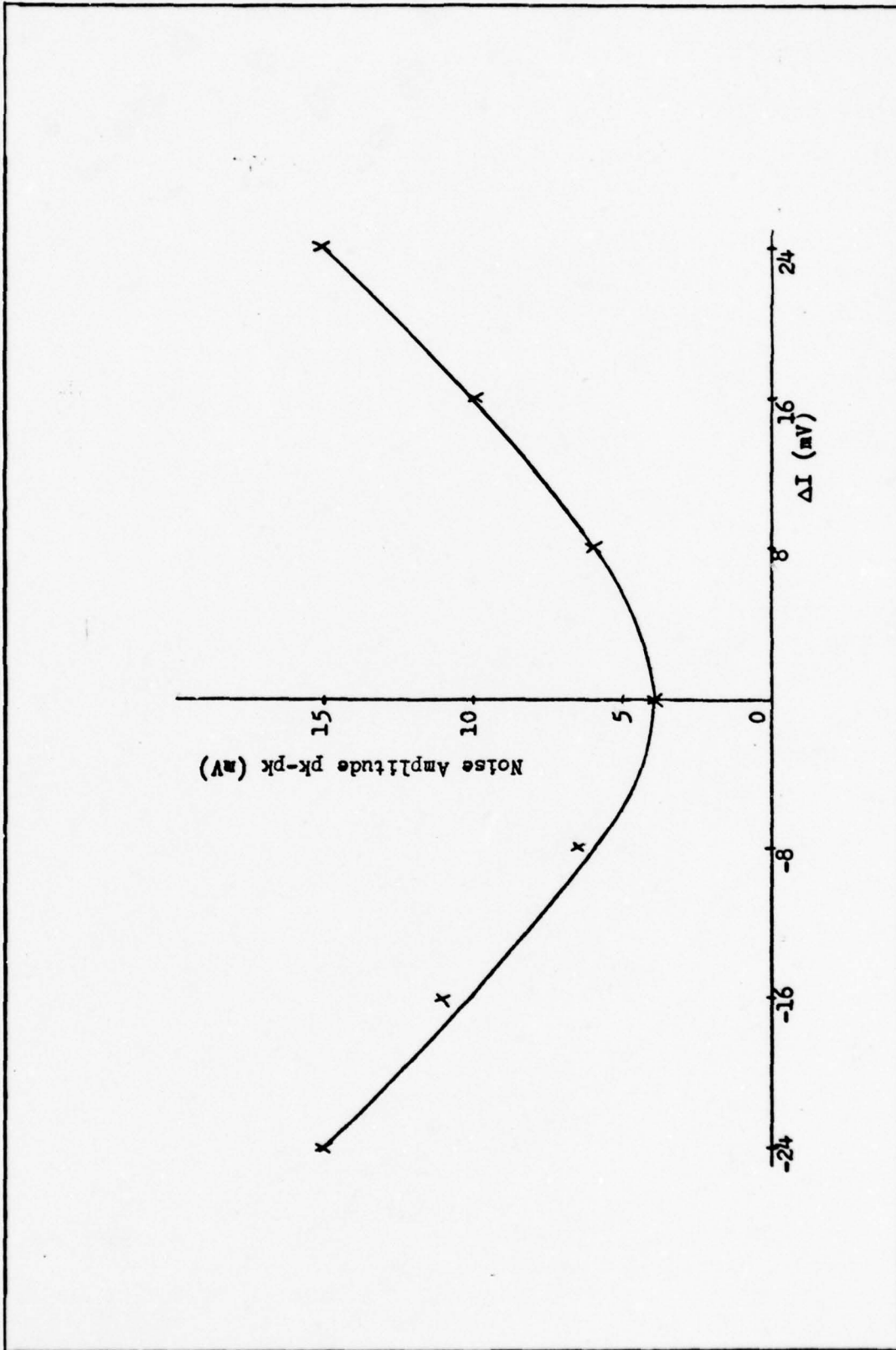
Figure 3.5 Noise Amplitude Versus ΔI

range of HVA bias voltage on the PZT. Additional sets of bias voltages could be obtained by then adjusting the laser frequency and rerunning the same series of tests. Prior to each run the intensity difference, ΔI, was checked to insure that the bias changes were not due to ΔI variations. The results of four separate runs are presented in Figure 3.6. The graph shows the non-linear responses associated with operating the HVA at either end of the 0-1000 volts dynamic range compared to the linear response at the center range value. Throughout the test the temperature was changed over a range from $56^{\circ}C$ to $57.5^{\circ}C$ and correspondingly the response curves moved to the left. Therefore, the best operation of the system occurs when the circuits are locked at the center of the dynamic range where, even if temperature changes are present, the response would still occur in the linear portion of the curve. These tests clearly indicate a need to change the method by which the cavity length is controlled.

Discussion

The most significant problem dealt with throughout this effort was temperature stabilization. The magnitude of this problem becomes apparent when the effect of temperature on the cavity is studied.

The coefficient of thermal expansion of the aluminum used for the cavity is 23.4 nm/mm/$^{\circ}C$. Now, assuming equal expansion in both directions and using 17.5 cm as the length of one side of the beam path, the change in path length per $1^{\circ}C$ change in temperature is

$$4 \times 23.4 \times 175 = 0.0164 \text{ mm} = 26\lambda$$

the equivalent Δf in Hz can be found by using

$$\Delta f = c\Delta L/\lambda L = (3\times10^{10}\text{cm/sec} \times 26\lambda)/(\lambda \times 4 \times 17.5\text{cm}) = 1.11\times10^{10}\text{Hz}$$
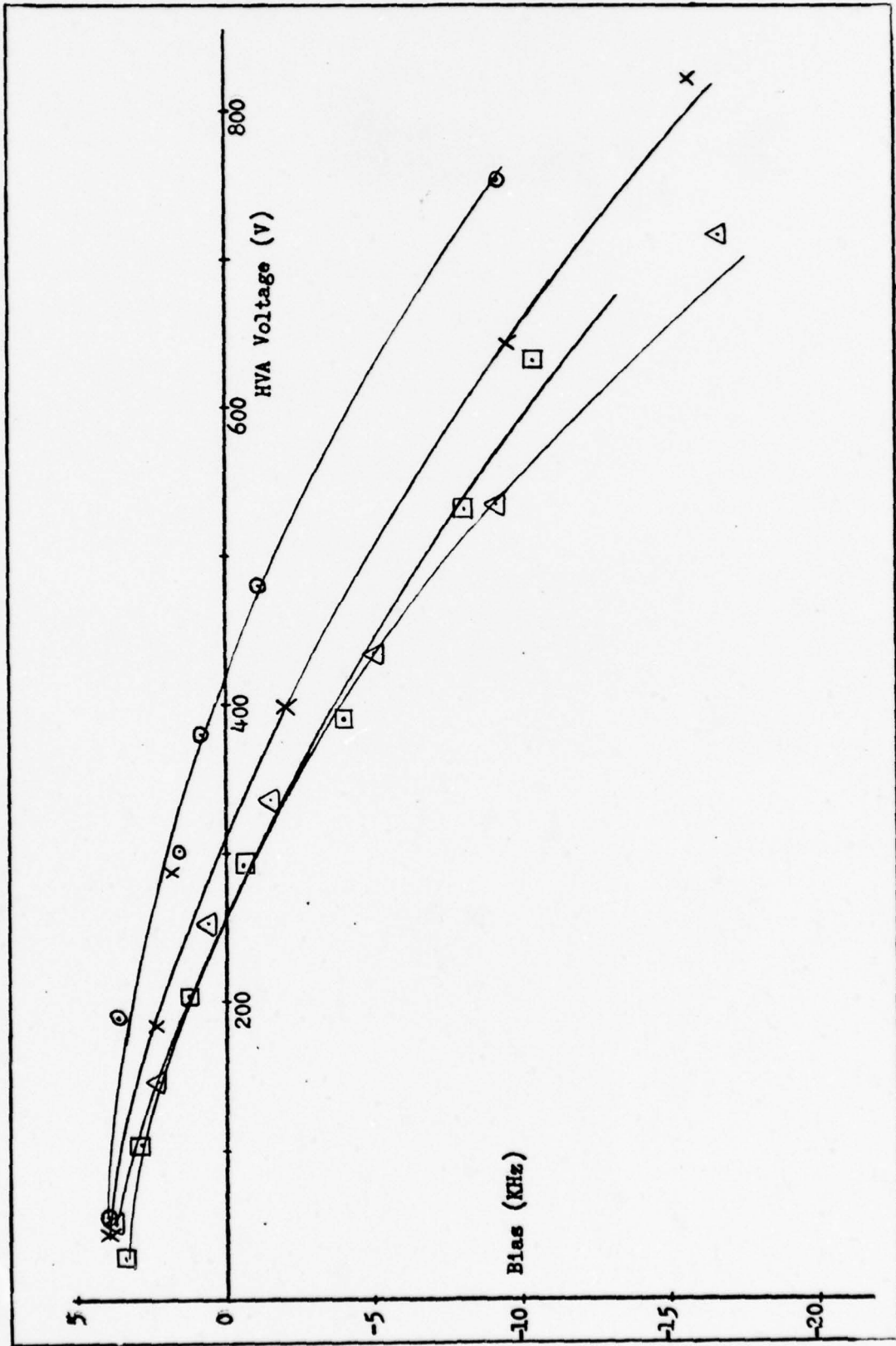
Figure 3.6 Gyro Bias Versus HVA Bias Output

The cavity loop compensates for this change in path length; however, the maximum path length change that can be obtained by full travel of the PZT is only 15.8λ or 6.77 x 10^9 Hz. Therefore, if thermal equilibrium is not reached during the performance test, the cavity loop integrator saturates quickly and, therefore, this effect is the limiting factor in test length. This indicates a need to either control temperature or redesign the PRLG to make it less sensitive to temperature. A further problem with temperature changes is misalignment which has already been shown to cause bias changes.

Figure 3.7 shows the effect of misalignment on intensity of each beam and ΔI. Note that due to misalignment, the modal structure of the cavity is different between the two directions. This results in the peaks present in the ΔI graph as the cavity is slow scanned. If the cavity were perfectly aligned, ΔI would appear as a straight line. As shown in the test results, ΔI causes the bias to change and also increases the noise within the rate loop. This also has an effect on long term bias stability and inertial rotation measurements as seen by the data. Additionally, the frequency drift, which resulted from the temperature changes, may also affect the system, though none should be expected if the cavity is perfectly aligned.

Even with the misalignment present, however, the PRLG detected rotation and showed the advantage of using the difference of the intensity signals to obtain the output. The performance results of the effect of ΔI on noise show that a 16 to 1 reduction in noise is obtained when the intensity signals are differenced. Further, by using ΔI as an input to the system, an improvement can be made to lessen the noise output. This will be discussed in the next chapter.
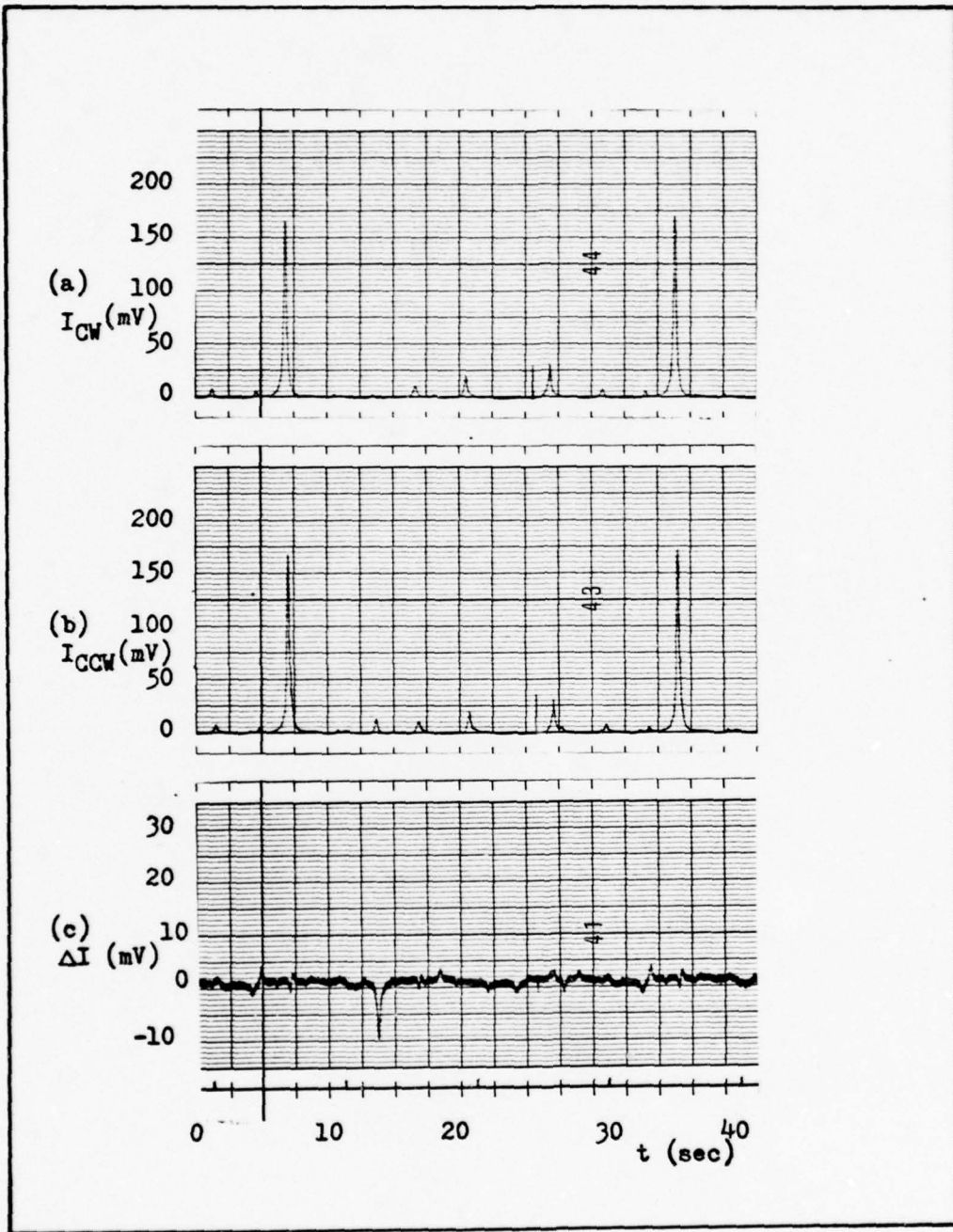
38

Figure 3.7 Effect of Misalignment of Intensity and ΔI (a) I_{CW} (b) I_{CCW} (c) ΔI

IV Conclusions and Recommendations

Conclusions

The first, foremost and most extensive task of this project was to fabricate and check out a passive ring resonator laser gyroscope. As a result, these pages have presented a detailed explanation of this new rotation sensing method to include a description and operation of the system. The data obtained through the various tests showed the relative merit of the concept and proved that the gyro can measure rotation rates in the lock-in region without concern for the problems normally associated with the typical active ring laser gyro. Two sources of error were found, namely nonlinearities within the PZT and differences between CW and CCW input intensities. It was shown that by using the difference in the output intensities as the control input to the rate loop, a significant reduction in noise was obtained. It was also shown that, although a bias stability of 100 Hz over 36 minutes was obtained, low frequency noise on the system output is a severe problem. While it was not possible in the time available to touch upon all of the performance characteristics, it is hoped that this effort will provide a basis for continued research in this area. As for all new systems, there are limitations and shortcomings to which all experimenters have to cope. This project was no different, but data results did prove the validity of the method. To aid further research, a detailed list of recommendations will follow for consideration and adaptation in ongoing experiments.

Recommendations

The problems encountered during this study plus the novelty of

this approach to inertial rotation lend themselves to the formulation of several recommendations. These have been divided into four areas: environmental, mechanical, electronic, and experimental. They are presented in this order.

Environmental. As seen in Chapter III, temperature control was the biggest problem encountered. The ideal situation is to operate within a small room which is equipped with its own temperature control system. This would allow the system to operate without an insulating covering thus allowing easier access for adjustments and preventing sudden temperature changes. If this is not possible, a temperature control circuit which responds quickly to changes in room temperature should be used. This would require an insulating covering over the PRLG. Also, by positioning the laser power supply ballast resistor outside of this covering, better control and lower temperatures would be obtained. Another way to reduce the temperature sensitivity of the system would be to make the resonant cavity out of a low thermal coefficient of expansion metal such as Invar.

Mechanical. The alignment of the system was accomplished using spring adjustable mirrors. This introduced noise because air currents and sound vibrations affected the output, sometimes to the point where the cavity lock was broken. Therefore, it is recommended that the mirror mounts be replaced with mounts that are shimmed into alignment. This can be done relatively easily by aligning the system with the present spring adjustable mounts and then replacing the mounts one at a time, ensuring that the system is aligned between each replacement. If the convenience of the adjustable mounts is desired, the mounts can be modified to lock them in place with set screws.

41

Further mechanical stability can be obtained by mounting an aluminum plate over the entire assembly connecting all of the components. In designing the hardware for this system, extra holes were drilled and tapped to accomodate this modification.

Because of the nonlinearity observed in the PZT, a different PZT should be used which provides a longer linear range and one that can be driven at higher modulation frequencies to improve the noise characteristics. This would allow a larger system bandpass for better control over the cavity. By using a shorter PZT, these advantages would be realized. However, a smaller dynamic range would result so that drift due to cavity length changes would have to be proportionally decreased.

Electronic. Several recommendations dealing with the electronics of the system can be made.

Temperature and/or mechanically induced changes in the laser cavity causes the single frequency mode within the gain curve to drift causing the input light to the resonant cavity to vary in frequency and intensity. If there is misalignment present within the cavity, these changes will affect the output. For this reason, a circuit which locks the laser mode to the top of the gain curve utilizing the same phase sensitive detection technique used in the cavity loop is recommended to be added to the system. This circuit will allow control of over two more variables when cause and effect studies of other variables are made. This, in fact, was attempted at first in this study. However, HVA noise plus optical feedback into the laser prevented this circuit from working well enough to be used. By using an HVA with better noise characteristics and by using a polarizer-quarter wave plate assembly (an isolation element) in the cavity external light path, a frequency stable light source can be obtained.

42

A final recommendation of this type is to use the ΔI signal to control the output signal amplitude of the VCO. Based upon the results for the tests finding the variations in bias and noise due to ΔI, which show that there is a minimum noise position for ΔI and that any change in ΔI also changes the bias, then by maintaining the ΔI signal at its minimum noise position, the effects of cavity misalignment, which causes a non rotationally induced error in the rate loop, will be decreased. Also, the noise content of the error signal used by the rate loop will be minimized. Again, this action would allow control over one more variable when analyzing system performance.

Experimental. From the data, it is seen that PZT position, intensity variations, and temperature affect the output of the PRLG either through noise or bias changes. Throughout these experiments the output frequency and intensity of the laser were kept relatively constant. A future experiment would be an investigation of how the gyro output is affected by laser intensity and frequency variations. Another variable that may affect the output is the polarization plane of the laser light. Throughout these experiments, the polarization plane was not altered.

Finally, the reduction of optical elements, and hence, noise sources, can be obtained by using two outputs of the laser and by using a triangular or rectangular shaped resonant cavity. The basic designs, as proposed by S. R. Balsamo, are shown in Figures 4.1 and 4.2. These designs would be expected to reduce errors due to misalignment, energy loss due to backscattering at mirror surfaces, and changes in polarization due to reflection.
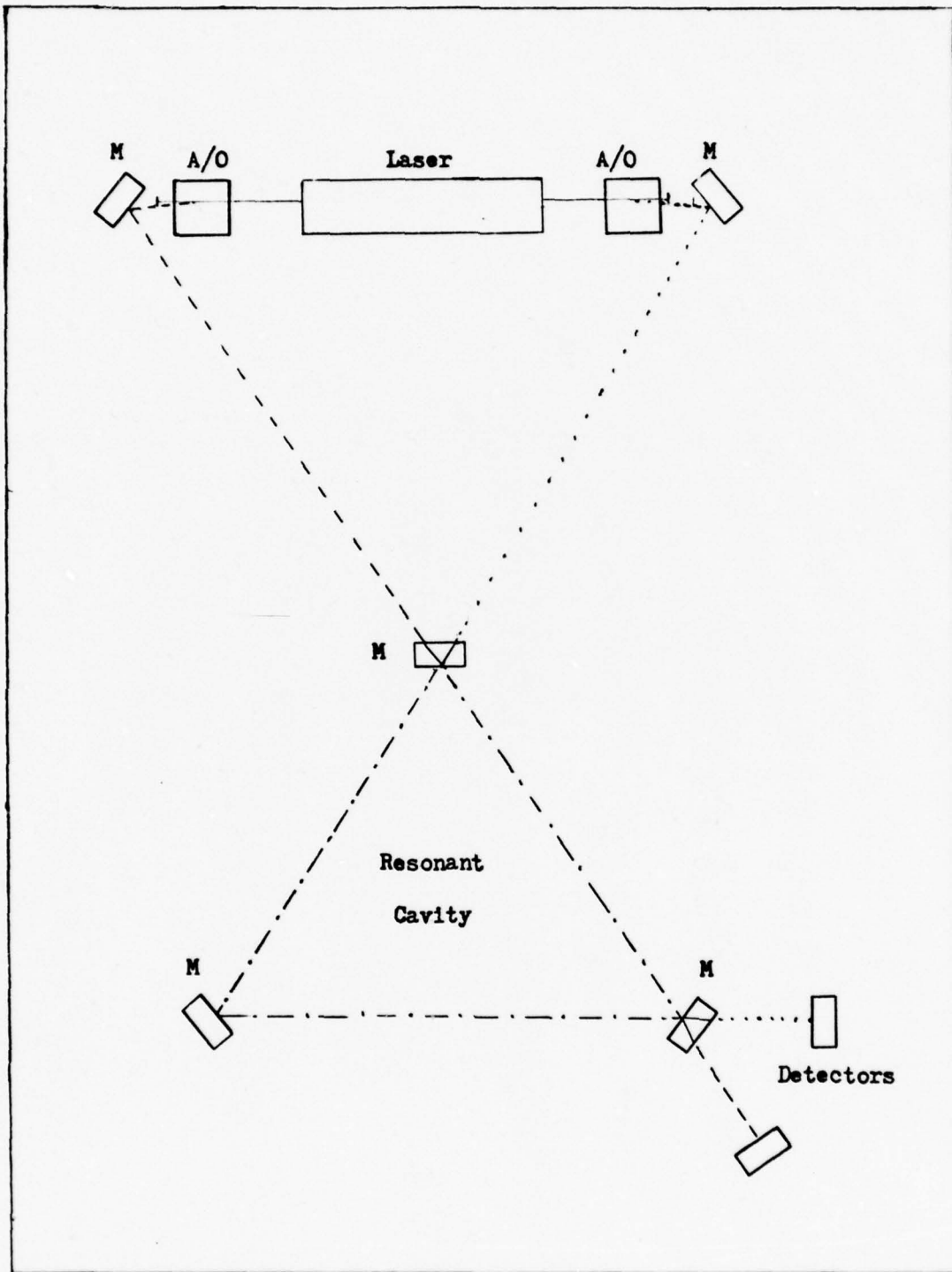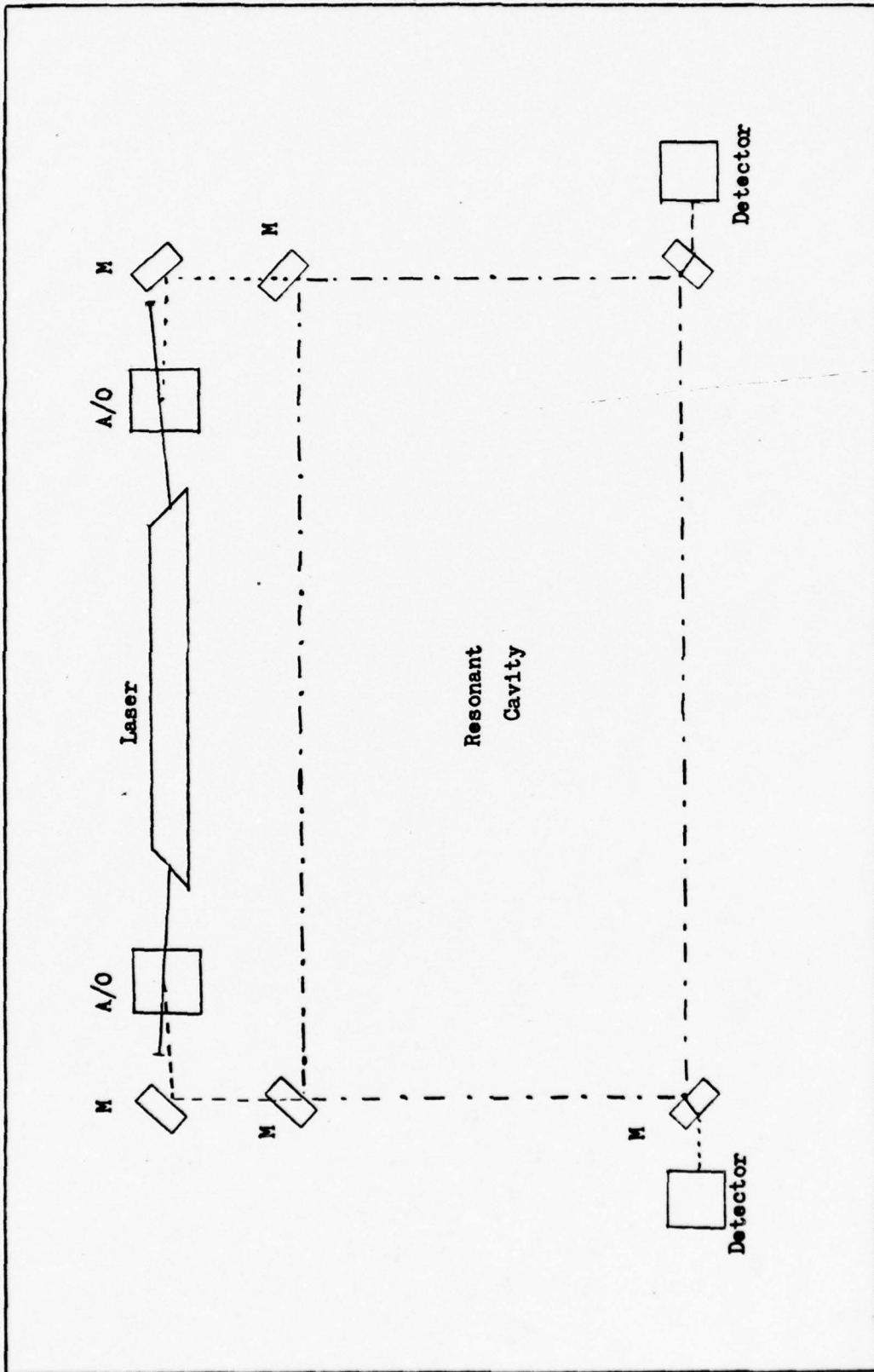
43

Figure 4.1   Minimum Optical Element PRG

44

Figure 4.2 Reduced Optical Element PRG

45

Bibliography

1. Sagnac, G. Computes Rendus Acadamie Des Sciences (Paris), 157: 708 (1913); 157: 1410(1913).

2. Ezekiel, S. and Balsamo, S. R. "Passive Ring Resonator Laser Gyroscope," Applied Physics Letters, 30: 478-480 (May 1977).

3. Greenstein, H. "Progress on Laser Gyros Stimulates New Interest," Laser Focus, (February 1978).

4. 7040-3332. The Honeywell Laser Gyro. Government and Aeronautical Products Division, Minneapolis, Minnesota.

5. Aronowitz, F. Laser Applications, Vol 1. New York: Academic Press Inc., 1971.

6. Rosenthal, Adolph H. "Regenerative Circulatory Multiple-Beam Interferometry for the Study of Light-Propagation Effects," Journal of the Optical Society of America, 52: 1143-1148 (October 1962).

7. Macek, W. M. and Davis, Jr., D. T. M. "Rotation Rate Sensing with Traveling-Wave Ring Lasers, "Applied Physics Letters, 2: 67-68 (February 1963).

8. Yariv, Ammon. Introduction to Optical Electronics. New York: Holt, Rinehart and Winston, 1976.

Appendix A: Description of the Modulation Technique

The generation of an error signal used to drive the cavity length to the resonance condition is based upon modulating the length of the cavity such that the intensity of light out of the cavity is also modulated dependent upon the length of the cavity relative to the resonance condition.

If the intensity alone were used as an error signal then the variation of I from I_{MAX} is an excellent indication of how far the cavity must be moved to bring it in resonance. Unfortunately, that signal alone is insufficient because there is no information to indicate in which direction the cavity length must be moved to return it to resonance. By modulating the cavity at a frequency at least a factor of two higher than the bandwidth required for the control loop, an error signal can be generated which is both indicative of the amount of error and the direction.

The method of operation can be best explained with reference to Figure A.1. With the cavity such that it is in resonance with the incident light frequency, the cavity would be in position A of Figure A.1. The modulation voltage (V_m) dithers the cavity length such that the intensity detector output is as shown in Figure A.2. These two signals are then mixed such that the output of the mixer (actually a cross correlation detector) can be viewed as the product of the two input signals. Thus the output of the mixer, called a phase sensitive detector, is a sinusoidal in this case as shown in Figure A.2. This signal is then low pass filtered to produce a zero DC level output indicating that the cavity is indeed on resonance.
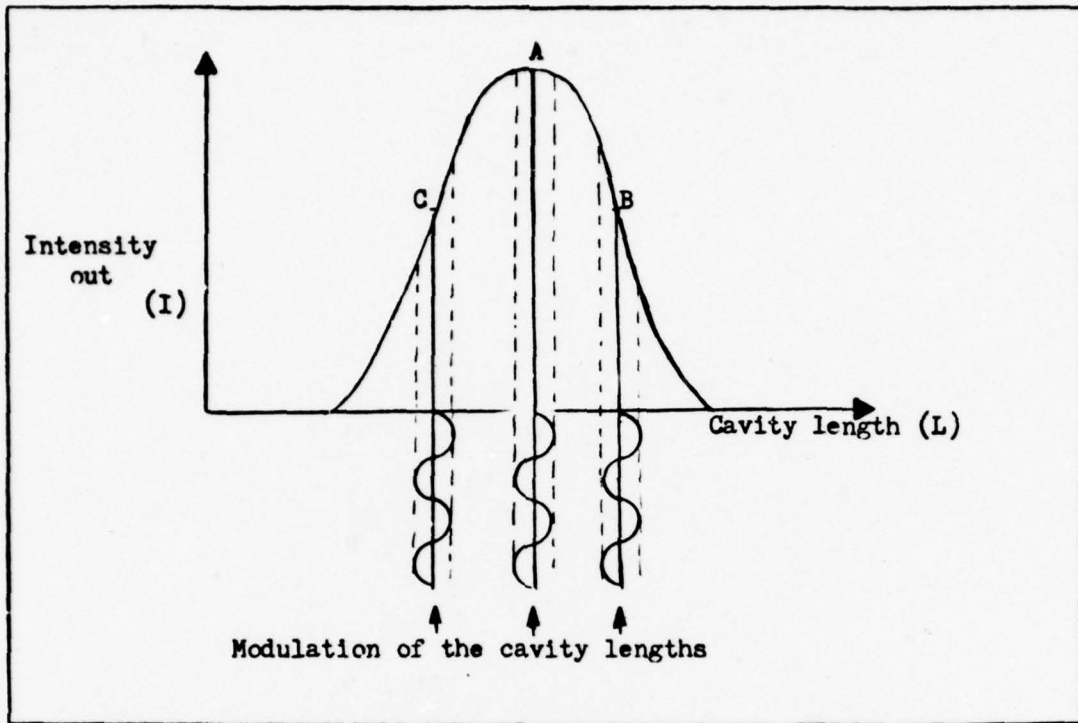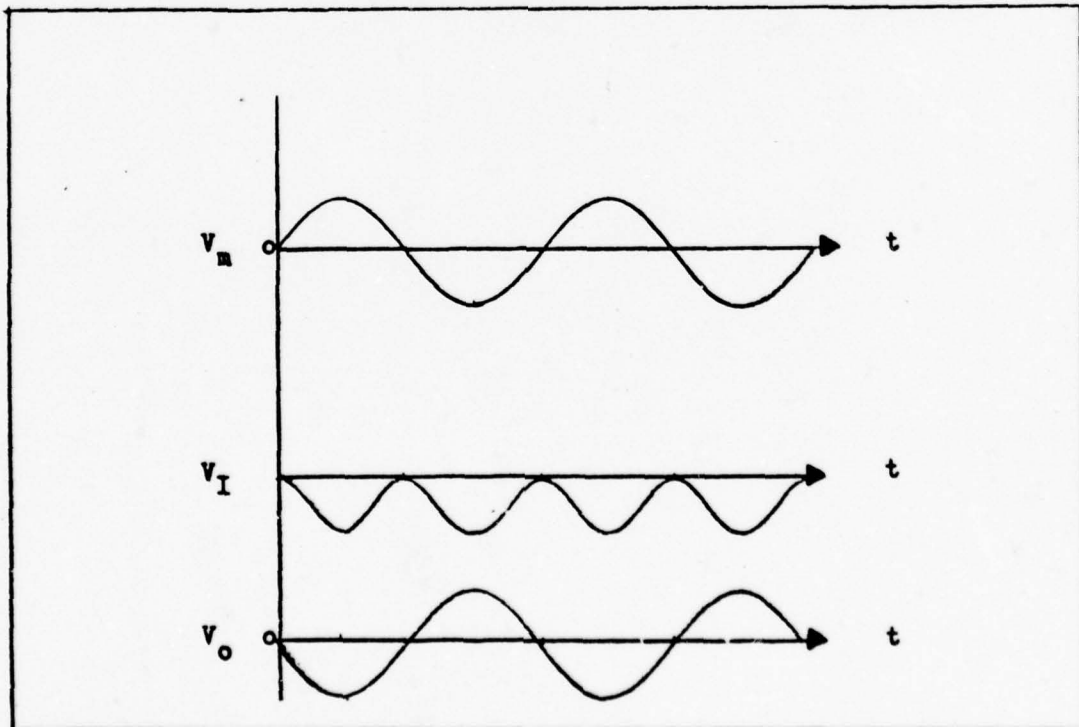
47

Figure A.1 I Versus L

Figure A.2 Modulation Signal, V_m; Detector Output, V_I; and PSD Signal Output, V_o; at Resonance

For the case when the cavity is longer than required for the resonance condition refer to position B of Figure A.1. In this case the intensity detector output voltage is out of phase with the modulation signal and when multiplied produces a net negative signal (see Figure A.3). Again when low pass filtered, a negative voltage is generated indicating that the cavity must be shortened.

Finally for the case when the cavity is shorter than required, the situation is as shown in position C of Figure A.1 and the phase sensitive dector output voltage is as shown in Figure A.4. The phase sensitive detector output voltage in this case is positive indicating a need to increase the cavity length.

The technique described here is also used to derive the error signal necessary to adjust the acousto-optic driving frequency such that the frequency of the incident light in that loop is in resonance with the cavity.
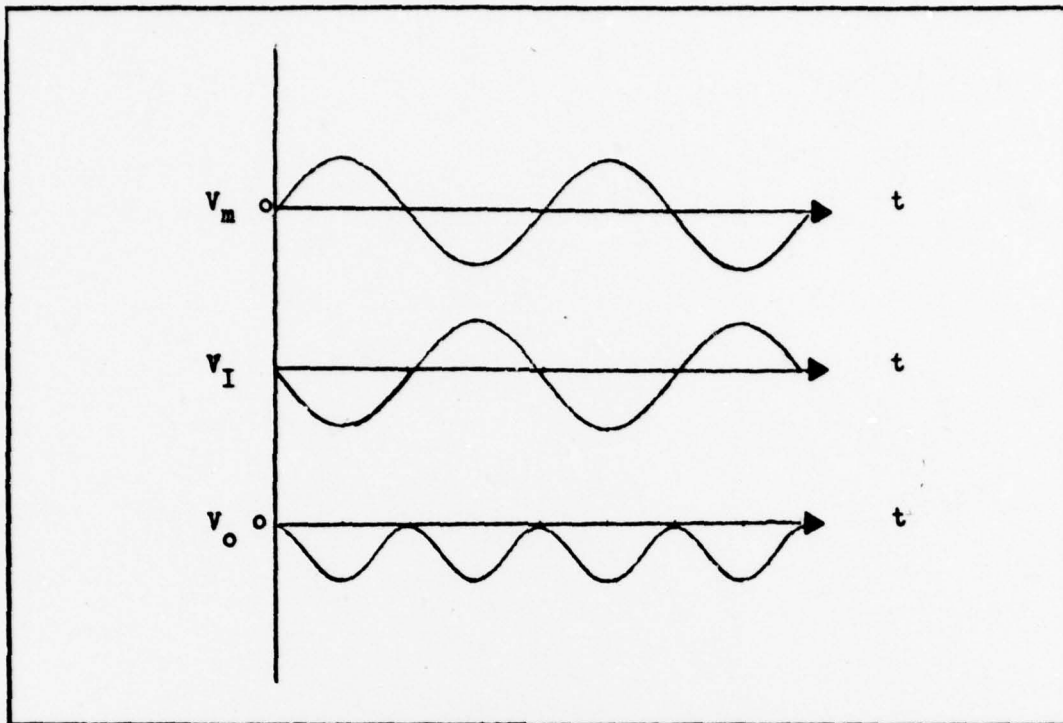
Figure A.3 Modulation Signal, V_m; Detector Output, V_I; and PSD Signal Output, V_o; with Cavity Length Longer than Resonant Length
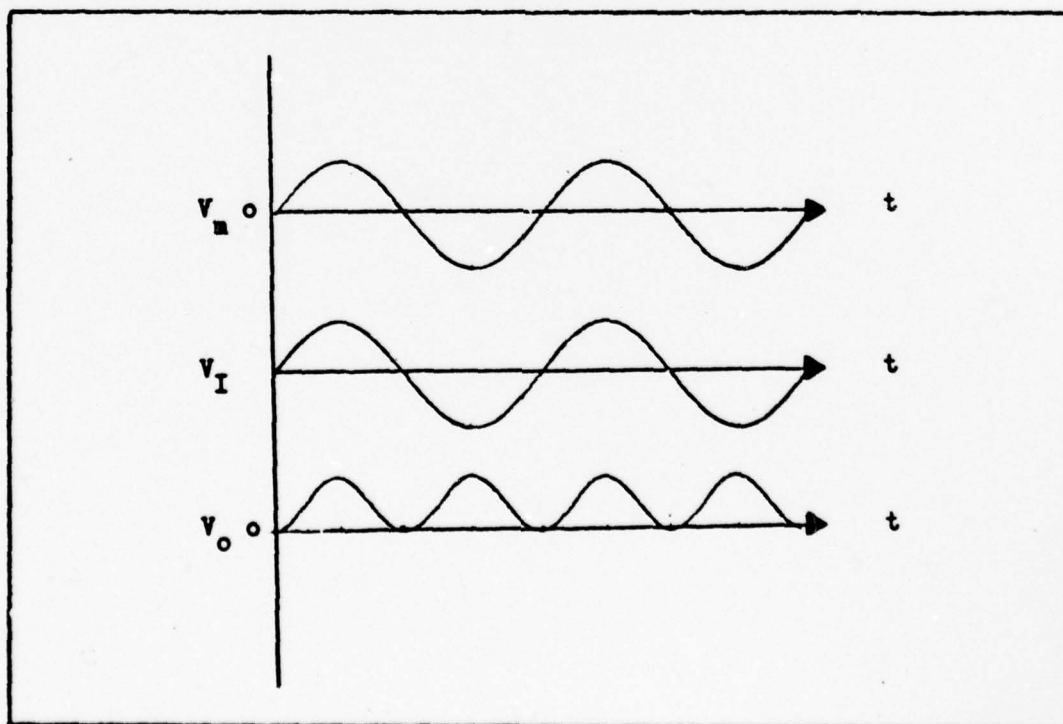

Figure A.4 Modulation Signal, V_m; Detector Output, V_I; and PSD Signal Output, V_o; with Cavity Length Shorter than Resonant Length

Appendix B: Experimental Procedure

Laboratory Test Set-up

The laboratory and test site used in this experiment is located in the Air Force Institute of Technology Building 640, Room 238 at Wright Patterson AFB, Ohio. The geographical coordinates of this location are 39° 47' 17'' North latitude and 84° 05' 45'' West longitude at an elevation of 830 feet above mean sea level. Within the laboratory the PRLG is mounted on a Genisco Rate of Turn Table. To reduce the effects of high frequency oscillations, a 13.5 cm layer of foam is placed between the gyro mount and the rate table. The associated electronic equipment for the PRLG is situated in racks on either side of the gyro. Figure B.1 shows the laboratory set-up for the gyro.

Figure B.1 PRLG with Associated Electrical Equipment

51

The equipment which is critical to the experiment and requires a significant time for warm up is continually powered throughout the data gathering process. These components include the laser, lock-in amplifiers, frequency synthesizer, and the voltage control oscillator. To reduce the temperature variations within the lab, the air conditioning system is shut off and the entrance to the room is closed. This action stabilizes the temperature within one degree of $23^{\circ}C$. Also a plastic mount is placed over the PRLG to reduce any wind motion effects on the light waves.

For data gathering, selected outputs are connected to a chart recorder. These outputs include signals from the light intensity detectors, lock-in amplifiers, compensator circuits, and the voltage control oscillator. The light detector outputs are routed separately to their respective 10 gain amplifiers in order that the intensity of the CW and CCW beams can be monitored within the sensitivity range of the recorder. In addition, the detector signals are connected to a 100 gain differential amplifier so that the difference in the signal can be displayed. The voltage control oscillator provides the signal to the frequency counter which displays a visual output for the frequency value of f_2. Additionally, the frequency counter provides a signal to the chart recorder. This is accomplished by routing the frequency counter signal thru an electronic digital counter to a digital/analogue (D/A) converter which converts the digital output to a signal which is compatible to the input required for the recorder. Also, the D/A circuit allows the operator the convenience of selecting which grouping of the last five digits of f_2 necessary for display purposes (5,4,3/4,3,2/3,2,1). Then, to obtain the differences in the CW and CCW resonance frequencies, f_2 is subtracted from 40 MHz. Finally, the outputs of the cavity and

52

the rate lock-in amplifiers and compensators are connected to the recorder for monitoring. Figure B.2 summarizes the data recording process.
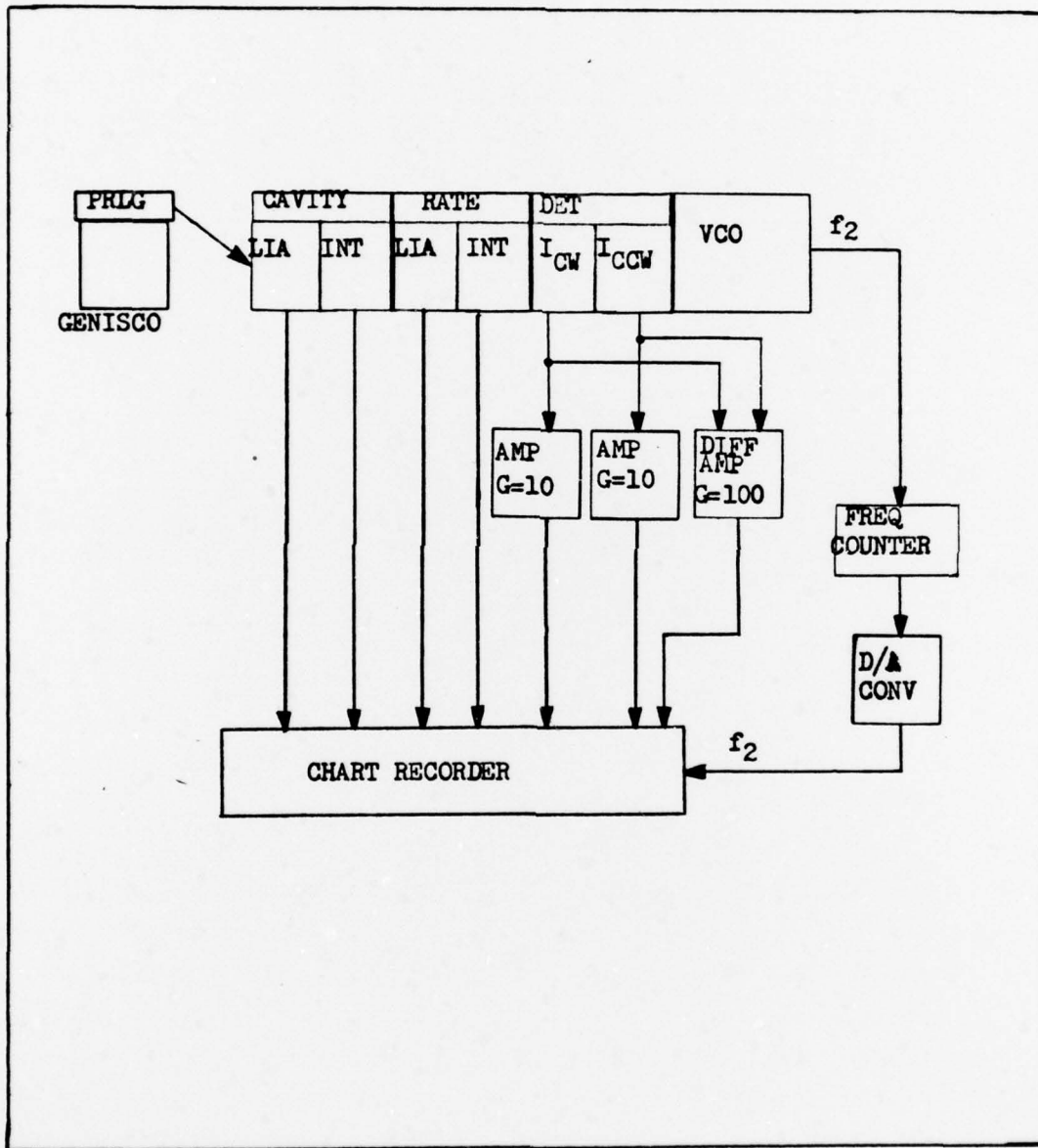

Figure B.2 Data Recording Diagram

53

Test Procedure

To obtain meaningful data, all tests need to be initiated from a standarized setting of performance parameters. This is accomplished in a sequence of events which provides an output with minimum noise within the limiting physical and electrical characteristics of the PRLG and the associated equipment. The following steps explain the test procedure used in this PRLG experiment and, if followed, provides a test standard from which to evaluate the desired data.

Step 1: Align the laser and adjust the mirror to obtain the maximum output.

Step 2: Align the resonant cavity in the CW and CCW directions to obtain maximum intensity in the laser beams. This is accomplished by applying a 150 volt sawtooth signal to the cavity PZT and scanning the laser modes. By first adjusting the mirrors in the CCW direction, the resonant cavity is aligned and the associated laser mode maximized. Then adjustments are made to the external mirrors in the CW direction to obtain the same result.

Step 3: Minimize the intensity difference between the two beams through the use of the output signal amplitude knob on the VCO which enables the CCW beam to be adjusted to the same intensity as the CW beam. (Due to efficiency differences in the acousto-optic frequency shifters and the beamsplitter, the two beams differ slightly in intensity.) The VCO output signal amplitude knob controls the acousto-optic driven power.

Step 4: Monitor the intensity difference, ΔI, and make minor adjustments to the external mirrors in the CW direction to reduce misalignment errors.

Step 5: Adjust the longitudinal mode of the laser to the top of the gain curve by applying a bias voltage to the PZT which holds one of the laser mirrors. While scanning the resonant cavity with the 150 volt sawtooth signal, display the output of each lock-in amplifier and minimize the signal by adjusting the phase switch then rotate the phase 90° to obtain the maximum derivative signal. This process reduces any errors caused by modulation of the PZT and oscillator which would otherwise generate an error signal independent of inertial rotation.

Step 6: With zero input to the compensator units, null out the integrator circuits. This is necessary because of internal temperature changes of the operational amplifier causing an unwanted input voltage to the integrator.

Step 7: Turn on the cavity compensator switches and short the integrator out with the 100 ohm resistor. This sets the integrator output to zero.

Step 8: Set the mode peak at the top of the gain curve and search for the proper pathlength at that mode by adjusting the HVA. When found, switch the 100 ohm resistor out of the circuit and the cavity loop locks to the maximum signal.

Step 9: Monitor the output error signal of the rate lock-in amplifier and minimize this signal (ΔI) through the use of the output signal amplitude knob on the VCO. This procedure sets ΔI at the minimum noise position for the start of the data run.

Step 10: Turn on the rate compensator switches. This action locks the circuit in the rate loop.

When the above procedure is completed, the type of experiment to be run is reviewed and the recording equipment is set accordingly. By

55

monitoring the outputs, the error signals and performance parameters can be immediately reviewed to determine if the system is operating within an allowable tolerance for a valid test run. If not, then the cause is isolated and a course of action is determined. Normally, adjustments in the compensator circuit (gain, lead, integration time) and lock-in amplifiers (time constant, sensitivities) can remedy the situation by reducing noise effects and providing a stronger signal for the locking sequence.

Appendix C: <u>Equipment Listing</u>

The following list of equipment was used in the PRLG experiment and the number of individual components used are so indicated.

Type of Equipment   Number Required

Acousto-optic Light Modulator, IntraAction Model AOM-40. 2

Chart Recorder, Gould Brush 200 eight channel. 1

DC Power Supply, Hewlett Packard Model 6274A 1

DC Power Supply, Powertec Model 6C3000. 1

Electronic Counter, Hewlett Packard Model 5248M. 1

High Voltage DC Op Amp, Burleigh Model PZ-70. 2

Laser Exciter, Spectra-Physics Model 249. 1

Lock-in Amplifier, Princeton Applied Research Model 124A 2

Mirrors, Dielectric

    Laser--1-Flat/100% Reflectivity,1-Curved/99% Reflectivity.. 2
    External Path--Flat/100% Reflective. 3
    Resonant Cavity--Curved/1m,2/100% & 2/99% Reflectivity . .4

Photodiode Light Detector, United Detector Tech Model PIN-6DP. . 2

Piezoelectric Length Transducer, Burleigh Model PZ-80. 2

Rate of Turn Table, Genisco Model C-181. 1

Signal Generator, Hewlett Packard Model 8640B. 1

Synthesizer Driver, Hewlett Packard Model 5110A. 1

Wideband Amplifier Module, R. F. Power Labs Model M305S. 2

Beamsplitter. 1

Compensator (see Figure D.1). 2

Gain Tube, CW Radiation Inc. 1

Pre-Amplifier for Light Detector (see Figure D.2). 2

Appendix D: Electrical Circuits

Figure D.1 is the electrical circuit diagram of the compensation
circuit used in the experiment. Figure D.2 is the diagram of the photo-
diode light detector and pre-amplifier circuit. These components were
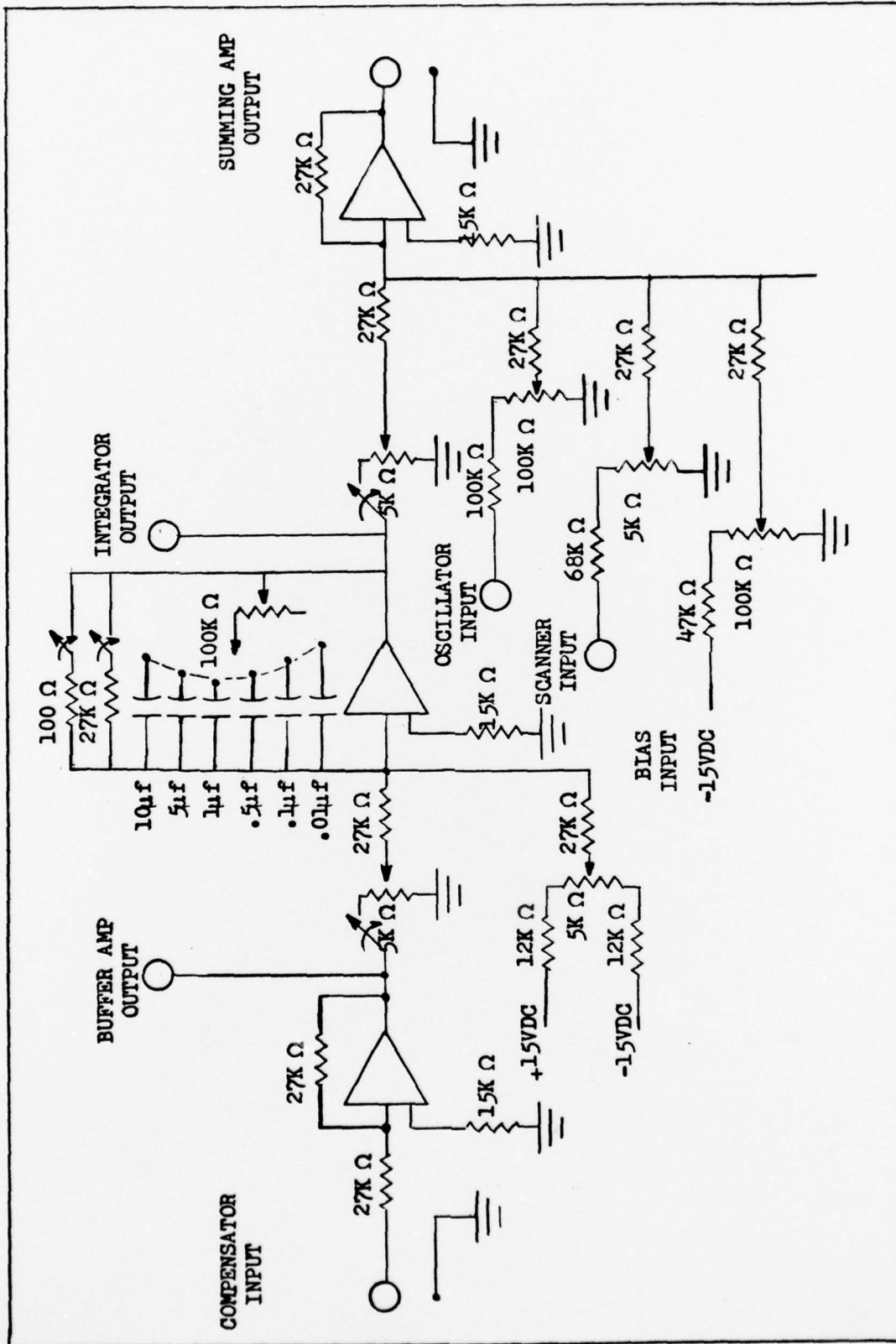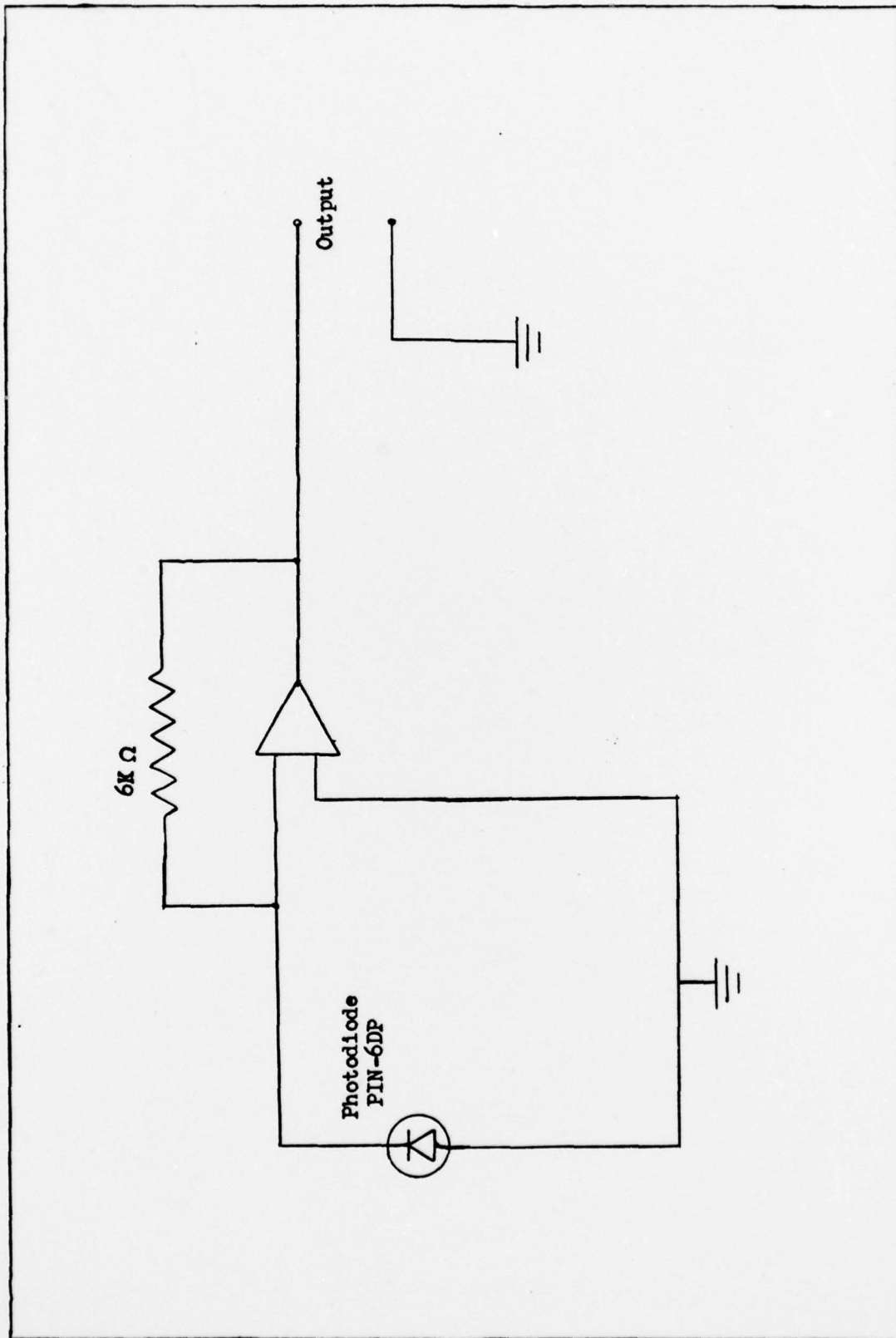fabricated and designed especially for the PRLG.

Figure D.1 Compensator Circuit

59

Figure D.2 Pre-Amplifier with Light Detector

Vita

Charles R. Holland was born on 21 January 1946 in Elkins, West Virginia. After graduation from Elkins High School, he attended West Virginia University for one year then transferred to the USAF Academy. In 1968, he graduated from the Academy with a Bachelor's Degree in Aeronautical Engineering. He graduated from pilot training the following year and was assigned to fly tactical airlift C-130s at Dyess AFB, Texas. After a tour in Thailand flying AC-130 gunships, he was assigned to Ramstein AB, Germany as an Air Operations Staff Officer with the Directorate of Airlift at Headquarters USAFE. Upon the consolidation of airlift under MAC, he was transferred to the Military Airlift Center Europe and performed duties as a MAJCOM Joint Training Exercise Planner. During this tour of duty, he obtained a Master's Degree in Business Management from Troy State University. In 1975, he was selected to attend the Air Force Institute of Technology from which he obtained a Master's Degree in Astronautical Engineering. He is currently assigned to the Space and Missile Systems Organization in Los Angeles, California. He is married and has one son.

David J. Olkowski was born on 1 June 1949 in Detroit, Michigan. He graduated from Pioneer High School in San Jose, California in 1967. In 1972, he graduated from the University of California, San Jose with a Bachelor's Degree in Aeronautical Maintenance. He was commissioned from AFROTC as a Distinguished Graduate in 1972. In February of 1973, he was assigned to duty as a Missile Launch Officer for the Minuteman III-CDB weapon system at Francis E. Warren AFB, Wyoming. During this tour of duty, he obtained a Master's Degree in Business Administration

from the University of Wyoming. He was selected to attend the Air Force
Institute of Technology in 1977 from which he obtained a Master's Degree
in Astronautical Engineering. He is currently assigned to HQ 6585 Test
Group at Holloman AFБ, New Mexico. He is married and has two sons.

SECURITY CLASSIFICATION OF THIS PAGE (When Data Entered)

REPORT DOCUMENTATION PAGE		READ INSTRUCTIONS BEFORE COMPLETING FORM
1. REPORT NUMBER AFIT/GA/EE/78-2	2. GOVT ACCESSION NO.	3. RECIPIENT'S CATALOG NUMBER
4. TITLE (and Subtitle) EVALUATION OF ERRORS IN A PASSIVE RING RESONATOR LASER GYROSCOPE		5. TYPE OF REPORT & PERIOD COVERED MS Thesis
		6. PERFORMING ORG. REPORT NUMBER
7. AUTHOR(s) David J. Olkowski, Captain USAF Charles R. Holland, Captain USAF		8. CONTRACT OR GRANT NUMBER(s)
9. PERFORMING ORGANIZATION NAME AND ADDRESS Air Force Institute of Technology Wright Patterson AFB, Ohio 45433		10. PROGRAM ELEMENT, PROJECT, TASK AREA & WORK UNIT NUMBERS (AFIT-EN)
11. CONTROLLING OFFICE NAME AND ADDRESS Air Force Avionics Laboratory/RWA-2 Wright-Patterson AFB OH 45433		12. REPORT DATE December 1978
		13. NUMBER OF PAGES 73
14. MONITORING AGENCY NAME & ADDRESS(if different from Controlling Office)		15. SECURITY CLASS. (of this report) Unclassified
		15a. DECLASSIFICATION/DOWNGRADING SCHEDULE

16. DISTRIBUTION STATEMENT (of this Report)

Approved for public release; distribution unlimited.

17. DISTRIBUTION STATEMENT (of the abstract entered in Block 20, if different from Report)

18. SUPPLEMENTARY NOTES
Approved for public release; IAW AFR 190-17

J. P. Hipps, Major USAF
Director of Information   1-23-79

19. KEY WORDS (Continue on reverse side if necessary and identify by block number)
Laser gyro
Resonance frequency
Passive ring laser gyro
Error sources in a passive ring laser gyro

20. ABSTRACT (Continue on reverse side if necessary and identify by block number)
The passive ring resonator laser gyroscope is a new approach to measuring inertial rotation. This approach is based upon the Sagnac effect and uses a passive ring Fabry-Perot interferometer as the rotation sensing element. This report contains the results of a series of tests which were accomplished on a passive ring resonator laser gyroscope. The report contains a detailed description of this device plus a description of each test performed. These tests include noise measurements, inertial rotation measurements, and bias measurements. The test results show that the relationship

DD FORM 1473   EDITION OF 1 NOV 65 IS OBSOLETE   UNCLASSIFIED
1 JAN 73

SECURITY CLASSIFICATION OF THIS PAGE (When Data Entered)

20.

between the output frequency and input rotation rate is linear and is consistent with previously published data indicating no lock-in problem. The output bias is shown to be affected by piezoelectric transducer position and by differences in intensity between the counter-rotating light beams. Additionally, the difference in intensity also is shown to affect the noise content of the output. These significant new results lead to a recommendation to improve the performance of this new type of gyroscope via the addition of an intensity feedback control loop. In addition, the distortion of the rotation sensing cavity due to length changes in a piezoelectric length transducer shows that a cavity made of a lower thermal coefficient of expansion material is necessary to minimize the size of the piezoelectric length transducer and, therefore, the distortion due to the transducer.